Diffusion toward non-overlapping partially reactive spherical traps: Fresh insights onto classic problems

Denis S Grebenkov

Diffusion toward non-overlapping partially reactive spherical traps: fresh insights onto classic problems

Denis S. Grebenkov*
Laboratoire de Physique de la Matière Condensée (UMR 7643), CNRS – Ecole Polytechnique, IP Paris, 91128 Palaiseau, France
(Dated: Received: May 28, 2020/ Revised version:)

Several classic problems for particles diffusing outside an arbitrary configuration of non-overlapping partially reactive spherical traps in three dimensions are revisited. For this purpose, we describe the generalized method of separation of variables for solving boundary value problems of the associated modified Helmholtz equation. In particular, we derive a semi-analytical solution for the Green function that is the key ingredient to determine various diffusion-reaction characteristics such as the survival probability, the first-passage time distribution, and the reaction rate. We also present modifications of the method to determine numerically or asymptotically the eigenvalues and eigenfunctions of the Laplace operator and of the Dirichlet-to-Neumann operator in such perforated domains. Some potential applications in chemical physics and biophysics are discussed, including diffusion-controlled reactions for mortal particles.

PACS numbers: 02.50.-r, 05.60.-k, 05.10.-a, 02.70.Rr
Keywords: modified Helmholtz equation, diffusion-controlled reactions, Laplace operator, addition theorems, Dirichlet-to-Neumann operator

I. INTRODUCTION

Diffusion-reaction processes in industrial chemical reactors, living cells, and biological tissues have been studied over many decades[1–5]. Diffusion toward spherical traps (or sinks) is an emblematic model of such processes that attracted a considerable attention among theoreticians[6–16]. In a basic setting, one considers the concentration of diffusing particles $c(\boldsymbol{x},t)$ that obeys diffusion equation in the complement Ω of the union of non-overlapping balls:

$$\frac{\partial}{\partial t}c(\boldsymbol{x},t) = D\nabla^2 c(\boldsymbol{x},t), \qquad (1)$$

where D is the diffusion coefficient, and ∇^2 is the Laplace operator. This equation is completed by an initial concentration profile, $c(\boldsymbol{x},t=0) = c_0(\boldsymbol{x})$, an appropriate boundary condition describing reactions on the boundary $\partial\Omega$, and the regularity condition $c(\boldsymbol{x},t) \to 0$ as $|\boldsymbol{x}| \to \infty$. Various arrangments of traps may account for spatial heterogeneities and help to elucidate the role of disorder onto reaction kinetics, in particular, onto the reaction rate[17–23]. More generally, reactive traps and passive spherical obstacles can be used as elementary "bricks" to build up model geometrical structures of porous media or macromolecules such as enzymes or proteins[24–31].

As explicit analytical solutions to Eq. (1) are in general not available, various mathematical tools and numerical techniques have been broadly used. For instance, Torquato and co-workers applied the variational principle to derive upper and lower bounds on the steady-state reaction rate[12–14]. Among numerical techniques, Monte Carlo simulations and finite-element methods were most often employed thanks to their flexibility and applicability to arbitrary confining domains (see[32–35] and references therein). In contrast, the generalized method of separation of variables (GMSV), also known as the (multipole) re-expansion method, exploits the intrinsic local symmetries of perforated domains and relies on the re-expansion (addition) theorems. This method was applied in different disciplines ranging from electrostatics to hydrodynamics and scattering theory[36–40]. In chemical physics, the GMSV for the Laplace equation was used to study steady-state diffusion and to compute the reaction rate in various configurations of traps[28–31,41–45]. In particular, a semi-analytical representation for the Green function of the Laplace equation was derived both in three-dimensional[31] and two-dimensional spaces[46], allowing one to access most steady-state characteristics of the diffusion-reaction process such as the reaction rate, the escape probability, the mean first-passage time, the residence time, and the harmonic measure density. However, these results are not applicable to transient time-dependent diffusion among traps, which is governed by diffusion equation. As the Laplace transform reduces Eq. (1) to the modified Helmholtz equation (see below), it would be natural to adapt the GMSV to this setting. While the GMSV for ordinary Helmholtz equation has been broadly employed in scattering theory[36–40], its applications to the modified Helmholtz equation seem to be much less studied[47,48].

In this paper, we employ re-expansion formulas in spherical domains to develop a general framework for solving boundary value problems for the modified Helmholtz equation with Robin boundary conditions (specified below). From the numerical point of view, the proposed method can be seen as an extension of Ref.[31] from the Laplace equation to the modified Helmholtz equation, as well an extension of Ref.[48] from exterior to interior domains. From the theoretical point of view, we derive a semi-analytical representation of the Green function for the modified Helmholtz equation which de-

termines most relevant characteristics of transient time-dependent diffusion. Moreover, we discuss how this method can be adapted to compute the eigenvalues and eigenfunctions of the Laplace operator and of the Dirichlet-to-Neumann operator in such perforated domains. To our knowledge, these spectral applications of the method are new.

The paper is organized as follows. Section II presents the GMSV and its applications to get the Green function (Sec. II B), the heat kernel (Sec. II C), the Laplacian spectrum (Sec. II D) and the spectrum of the Dirichlet-to-Neumann operator (Sec. II E). In Sec. III, we describe practical aspects of these results and their applications in chemical physics. In particular, we discuss first-passage properties (Sec. III A), stationary diffusion of mortal particles (Sec. III B), as well as advantages, limitations and further extensions of the method (Secs. III C, III D). Section IV concludes the paper. Appendices regroup technical derivations and some examples.

II. GENERAL FRAMEWORK

We consider diffusion outside the union of N non-overlapping balls $\Omega_1, \ldots, \Omega_N$ of radii R_i, centered at $\boldsymbol{x}_i$:

$$\Omega = \Omega_0 \setminus \bigcup_{i=1}^{N} \overline{\Omega}_i, \quad \Omega_i = \{\boldsymbol{x} \in \mathbb{R}^3 \ : \ |\boldsymbol{x} - \boldsymbol{x}_i| < R_i\}, \quad (2)$$

where Ω_0 is a ball of radius R_0, centered at the origin $\boldsymbol{x}_0 = 0$, that englobes all the balls: $\overline{\Omega}_i \subset \Omega_0$ for all i (Fig. 1). We allow R_0 to be infinite (i.e., $\Omega_0 = \mathbb{R}^3$) that describes an exterior problem, in which particles diffuse in an unbounded domain Ω and thus can escape at infinity. In turn, for any finite R_0, one deals with an interior problem of diffusion in a bounded domain Ω.

A. General boundary value problem

We first consider a general boundary value problem for the modified Helmholtz equation

$$(q^2 - \nabla^2) w(\boldsymbol{x}; q) = 0 \quad (\boldsymbol{x} \in \Omega), \quad (3a)$$

$$\left(a_i w + b_i R_i \frac{\partial w}{\partial \boldsymbol{n}} \right)\Big|_{\partial\Omega_i} = f_i \quad (i = 0, \ldots, N), \quad (3b)$$

where q is a nonnegative parameter*, $\partial/\partial \boldsymbol{n}$ is the normal derivative on the boundary $\partial\Omega = \cup_{i=0}^{N} \partial\Omega_i$, oriented outwards the domain Ω, f_i are given continuous functions on $\partial\Omega_i$, and a_i and b_i are nonnegative constants such that $a_i + b_i > 0$ (i.e., a_i and b_i cannot be simultaneously 0).

*While we focus on nonnegative q throughout the main text, the method is implemented for any complex q, see Appendix B 3.

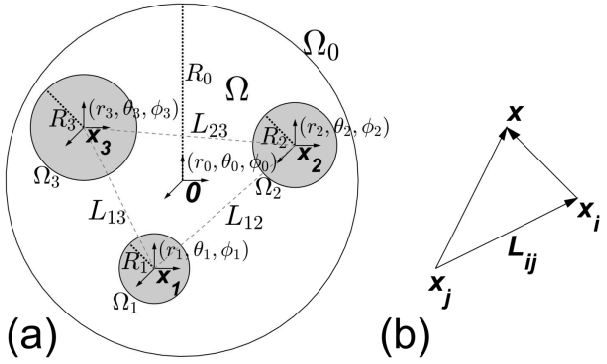

FIG. 1: **(a)** Illustration of a bounded perforated domain $\Omega = \Omega_0 \setminus \bigcup_{i=1}^{3} \overline{\Omega}_i$ with three balls Ω_i of radii R_i, centered at $\boldsymbol{x}_i$, all englobed inside a larger ball Ω_0 of radius R_0 centered at the origin. Local spherical coordinates, (r_i, θ_i, ϕ_i), are associated with each ball. The exterior problem corresponds to the limit $R_0 = \infty$ when $\Omega_0 = \mathbb{R}^3$. **(b)** Any point $\boldsymbol{x}$ can be represented either in local spherical coordinates (r_j, θ_j, ϕ_j), associated with the center $\boldsymbol{x}_j$, or in local spherical coordinates (r_i, θ_i, ϕ_i), associated with the center $\boldsymbol{x}_i$. Accordingly, basis functions $\psi^{\pm}_{mn}(\boldsymbol{x} - \boldsymbol{x}_j)$ can be re-expanded on basis functions $\psi^{\pm}_{kl}(\boldsymbol{x} - \boldsymbol{x}_i)$, where $\boldsymbol{x} - \boldsymbol{x}_j = \boldsymbol{L}_{ij} + (\boldsymbol{x} - \boldsymbol{x}_i)$, with $\boldsymbol{L}_{ij} = \boldsymbol{x}_i - \boldsymbol{x}_j$ being the vector connecting $\boldsymbol{x}_j$ to $\boldsymbol{x}_i$.

The Robin boundary condition (3b) is reduced to Dirichlet condition for $b_i = 0$ and to Neumann condition for $a_i = 0$. In particular, our description can accommodate perfectly reactive traps or sinks ($a_i > 0$, $b_i = 0$), partially reactive traps ($a_i > 0$, $b_i > 0$), and passive reflecting obstacles ($a_i = 0$, $b_i > 0$). For the exterior problem, Eq. (3b) for $i = 0$ is replaced by the regularity condition $w(\boldsymbol{x}; q) \to 0$ as $|\boldsymbol{x}| \to \infty$.

The basic idea of the GMSV consists in searching for the solution of Eq. (3a) as a superposition of partial solutions w_i in the exterior of each ball $\Omega_1, \ldots, \Omega_N$, and in the interior of Ω_0:

$$w(\boldsymbol{x}; q) = \sum_{i=0}^{N} w_i(\boldsymbol{x}; q) \quad (4)$$

(for the exterior problem, $w_0 \equiv 0$). As each domain Ω_i is spherical, the corresponding partial solution can be searched in the *local* spherical coordinates (r_i, θ_i, ϕ_i) associated with Ω_i, as an expansion over regular (for $i = 0$) and irregular (for $i > 0$) basis functions $\psi^{\pm}_{mn}$ with unknown coefficients A^i_{mn},

$$w_i(\boldsymbol{x}; q) = \sum_{n=0}^{\infty} \sum_{m=-n}^{n} A^i_{mn} \, \psi^{\epsilon_i}_{mn}(q r_i, \theta_i, \phi_i), \quad (5)$$

where we use a shortcut notation $\epsilon_i = -$ for $i > 0$, and $\epsilon_0 = +$. For the modified Helmholtz equation, the basis functions are

$$\begin{aligned} \psi^{+}_{mn}(q r_i, \theta_i, \phi_i) &= i_n(q r_i) \, Y_{mn}(\theta_i, \phi_i), \\ \psi^{-}_{mn}(q r_i, \theta_i, \phi_i) &= k_n(q r_i) \, Y_{mn}(\theta_i, \phi_i), \end{aligned} \quad (6)$$

where

$$i_n(z) = \sqrt{\pi/(2z)}\, I_{n+1/2}(z), \qquad k_n(z) = \sqrt{2/(\pi z)}\, K_{n+1/2}(z) \tag{7}$$

are the modified spherical Bessel functions of the first and second kind, and $Y_{mn}(\theta,\phi)$ are the normalized spherical harmonics:

$$Y_{mn}(\theta,\phi) = \sqrt{\frac{(2n+1)\,(n-m)!}{4\pi\,(n+m)!}}\, P_n^m(\cos\theta)\, e^{im\phi}, \tag{8}$$

with $P_n^m(z)$ being the associated Legendre polynomials (we use the convention that $Y_{mn}(\theta,\phi) \equiv 0$ for $|m| > n$).

The unknown coefficients A^i_{mn} are fixed by the boundary condition (3b) applied on each $\partial\Omega_i$:

$$f_i = \sum_{j=0}^{N} \sum_{m,n} A^j_{mn} \left(a_i + b_i R_i \frac{\partial}{\partial \boldsymbol{n}} \right) \psi^{\epsilon_j}_{mn}(q r_j, \theta_j, \phi_j) \Big|_{\partial\Omega_i}, \tag{9}$$

where $\sum_{m,n}$ is a shortcut notation for the sum over $n = 0, 1, 2, \ldots$ and $m = -n, -n+1, \ldots, n$. As spherical harmonics form a complete basis of the space $L_2(\partial\Omega_i)$, one can project this functional equation onto $Y_{kl}(\theta_i,\phi_i)$ to reduce it to an infinite system of linear algebraic equations on the coefficients A^j_{mn}:

$$F^i_{kl} = \sum_{j=0}^{N} \sum_{m,n} A^j_{mn}\, W^{j,i}_{mn,kl} \qquad \begin{cases} i = 0, 1, \ldots, N, \\ l = 0, 1, \ldots, \ |k| \le l, \end{cases} \tag{10}$$

where

$$W^{j,i}_{mn,kl} = \left(\left(a_i + b_i R_i \frac{\partial}{\partial \boldsymbol{n}} \right) \psi^{\epsilon_j}_{mn}(q r_j, \theta_j, \phi_j) \Big|_{\partial\Omega_i}, Y_{kl} \right)_{L_2(\partial\Omega_i)} \tag{11}$$

and

$$F^i_{kl} = (f_i, Y_{kl})_{L_2(\partial\Omega_i)}, \tag{12}$$

with the standard scalar product: $(f,g)_{L_2(\partial\Omega_i)} = \int_{\partial\Omega_i} d\boldsymbol{s}\, f(\boldsymbol{s})\, g^*(\boldsymbol{s})$, asterisk denoting the complex conjugate. Even though A^j_{mn}, F^i_{mn}, and $W^{j,i}_{mn,kl}$ involve many indices, one can re-order them to consider A^j_{mn} (resp., F^i_{mn}) as components of a (row) vector $\mathbf{A}$ (resp., $\mathbf{F}$), while $W^{j,i}_{mn,kl}$ as components of a matrix $\mathbf{W}$, so that Eq. (10) becomes a matrix equation:

$$\mathbf{F} = \mathbf{A}\mathbf{W}. \tag{13}$$

In Appendix A 2, we provide the explicit formulas for the matrix elements $W^{j,i}_{mn,kl}$, which depend only on q, on the positions and radii of the balls Ω_i, and on the parameters a_i and b_i. The derivation of these formulas relies on the re-expansion (addition) theorems for basis solutions $\psi^{\pm}_{mn}$ [49,50]. Truncating the infinite-dimensional matrix $\mathbf{W}$ and inverting it numerically yield a truncated set of coefficients A^j_{mn}. In this way, Eqs. (4, 5) provide a semi-analytical solution of the boundary value problem (3a, 3b), in which the dependence on $\boldsymbol{x}$ is analytical (via explicit basis functions $\psi^{\pm}_{mn}$), but the coefficients A^i_{mn} have to be obtained numerically from Eq. (13). A practical implementation of this method is summarized in Appendix B, whereas its advantages and limitations are discussed in Sec. III C.

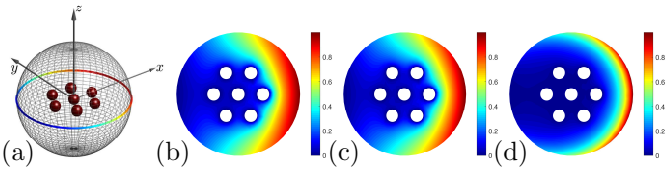

FIG. 2: **(a)** Configuration of 7 perfect traps of radius $R_i = 0.1$ inside a larger sphere of radius $R_0 = 1$ on which the variable concentration profile is set: $f_0(\theta,\phi) = \frac{1}{2}(1 + \sin\theta\cos\phi)$ (illustrated by a colored contour at the equator). **(b,c,d)** The solution $w(\boldsymbol{x};q)$ evaluated on a horizontal cut at $z = 0$ (i.e., in the plane xy, view from the top), with $q = 0.2$ **(b)**, $q = 1$ **(c)** and $q = 5$ **(d)**. The matrix $\mathbf{W}$ determining the coefficients A^i_{mn} was truncated to the size $8(3+1)^2 \times 8(3+1)^2 = 128 \times 128$ with the truncation order $n_{\max} = 3$.

Figure 2 illustrates three solutions $w(\boldsymbol{x};q)$ of the modified Helmholtz equation with Dirichlet boundary conditions on a configuration with 7 balls enclosed by a larger sphere. As q increases, the solution $w(\boldsymbol{x};q)$ drops faster from its larger values on the outer sphere toward the perfectly absorbing traps.

B. Green function

The above general solution allows one to derive many useful quantities. Here, we aim at finding the Green function $G(\boldsymbol{x},\boldsymbol{y};q)$ of the modified Helmholtz equation in Ω [51,52]

$$(q^2 - \nabla^2) G(\boldsymbol{x},\boldsymbol{y};q) = \delta(\boldsymbol{x}-\boldsymbol{y}) \quad (\boldsymbol{x} \in \Omega), \tag{14a}$$

$$\left(a_i G + b_i R_i \frac{\partial G}{\partial \boldsymbol{n}} \right) \Big|_{\partial\Omega_i} = 0 \quad (i = 0, \ldots, N), \tag{14b}$$

where $\delta(\boldsymbol{x}-\boldsymbol{y})$ is the Dirac distribution, and $\boldsymbol{y}$ is a fixed point in Ω (for the exterior problem, Eq. (14b) for $i = 0$ is replaced by regularity condition $G(\boldsymbol{x},\boldsymbol{y};q) \to 0$ as $|\boldsymbol{x}| \to \infty$). We search for the Green function in the form

$$G(\boldsymbol{x},\boldsymbol{y};q) = G_{\mathrm{f}}(\boldsymbol{x},\boldsymbol{y};q) - g(\boldsymbol{x};\boldsymbol{y},q), \tag{15}$$

where

$$G_{\mathrm{f}}(\boldsymbol{x},\boldsymbol{y};q) = \frac{\exp(-q|\boldsymbol{x}-\boldsymbol{y}|)}{4\pi|\boldsymbol{x}-\boldsymbol{y}|} \tag{16}$$

is the fundamental solution of the modified Helmholtz equation, whereas the auxiliary function $g(\boldsymbol{x};\boldsymbol{y},q)$ satis-

fies Eqs. (3), with

$$f_i = \left(a_i G_{\rm f} + b_i R_i \frac{\partial G_{\rm f}}{\partial \boldsymbol{n}} \right)\Big|_{\partial\Omega_i}. \qquad (17)$$

In Appendix A 3, we derive explicit formulas for the scalar product in Eq. (12) determining the components F^i_{mn} of the vector $\mathbf{F}$.

Among various applications, the Green function allows one to solve the inhomogeneous modified Helmholtz equation:

$$(q^2 - \nabla^2) w(\boldsymbol{x}; q) = F(\boldsymbol{x}) \quad (\boldsymbol{x} \in \Omega), \qquad (18a)$$

$$\left(a_i w + b_i R_i \frac{\partial w}{\partial \boldsymbol{n}} \right)\Big|_{\partial\Omega_i} = 0 \quad (i = 0, \ldots, N) \qquad (18b)$$

(with a given continuous function F) as

$$w(\boldsymbol{x}) = \int\limits_{\Omega} d\boldsymbol{y}\, G(\boldsymbol{x}, \boldsymbol{y}; q)\, F(\boldsymbol{y}). \qquad (19)$$

Equivalently, Eqs. (18) could be solved by reduction to homogeneous Eqs. (3) with the help of the fundamental solution $G_{\rm f}(\boldsymbol{x}, \boldsymbol{y}; q)$.

C. Heat kernel

The solution of the modified Helmholtz equation opens a way to numerous applications in heat transfer and nonstationary diffusion. For instance, the Green function $G(\boldsymbol{x}, \boldsymbol{y}; q)$ is related to the Laplace transform of the heat kernel $P(\boldsymbol{x}, t|\boldsymbol{y})$ that satisfies the diffusion equation

$$\frac{\partial P(\boldsymbol{x}, t|\boldsymbol{y})}{\partial t} - D\nabla^2 P(\boldsymbol{x}, t|\boldsymbol{y}) = 0, \qquad (20a)$$

$$P(\boldsymbol{x}, t = 0|\boldsymbol{y}) = \delta(\boldsymbol{x} - \boldsymbol{y}), \qquad (20b)$$

$$\left(a_i P + b_i R_i \frac{\partial P}{\partial \boldsymbol{n}} \right)\Big|_{\partial\Omega_i} = 0 \qquad (20c)$$

(for the exterior problem, the Robin boundary condition on $\partial\Omega_0$ is replaced by the regularity condition $P \to 0$ as $|\boldsymbol{x}| \to \infty$). The heat kernel describes the likelihood of the event that a particle that started from a point $\boldsymbol{y}$ at time 0, is survived against surface reactions on $\partial\Omega$ and found in a vicinity of a point $\boldsymbol{x}$ at a later time t[53,54]. The Laplace transform of the diffusion equation yields the modified Helmholtz equation, so that

$$\int\limits_0^\infty dt\, e^{-pt}\, P(\boldsymbol{x}, t|\boldsymbol{y}) = \frac{1}{D}\, G(\boldsymbol{x}, \boldsymbol{y}; \sqrt{p/D}). \qquad (21)$$

D. Laplacian eigenvalues and eigenfunctions

Replacing q by iq transforms the modified Helmholtz equation (3a) to the ordinary Helmholtz equation:

$$(q^2 + \nabla^2) w(\boldsymbol{x}; q) = 0. \qquad (22)$$

As solutions of this equation by the GMSV were thoroughly studied in scattering theory[36–40], we do not discuss them here. However, we mention that the above method can also be adapted to compute the eigenvalues and eigenfunctions of the Laplace operator $-\nabla^2$ in a bounded domain Ω (i.e., with $R_0 < \infty$):

$$\nabla^2 u(\boldsymbol{x}) + \lambda u(\boldsymbol{x}) = 0 \quad (\boldsymbol{x} \in \Omega), \qquad (23a)$$

$$\left(a_i u + b_i R_i \frac{\partial u}{\partial \boldsymbol{n}} \right)\Big|_{\partial\Omega_i} = 0. \qquad (23b)$$

As Eq. (23a) is the ordinary Helmholtz equation, it is convenient to search for an eigenpair $(\lambda, u(\boldsymbol{x}))$ in the form

$$u(\boldsymbol{x}) = \sum_{j=0}^{N} \sum_{m,n} A^j_{mn}\, \psi^{\epsilon_j}_{mn}(qr_j, \theta_j, \phi_j), \qquad (24)$$

with $q = i\sqrt{\lambda}$. This is equivalent to setting $f_i \equiv 0$ and thus $\mathbf{F} \equiv 0$ in Eq. (13). The necessary and sufficient condition to satisfy the matrix equation $\mathbf{AW} = 0$ is

$$\det(\mathbf{W}) = 0. \qquad (25)$$

If $\{q_k\}$ is the set of the values of q at which this condition is satisfied, one gets the eigenvalues: $\lambda_k = -q_k^2$. From the general spectral theory, the Laplace operator in a bounded domain with Robin boundary conditions is known to have an infinitely many nonnegative eigenvalues growing to infinity so that all zeros q_k should lie on the imaginary axis. In practice, the matrix $\mathbf{W}$ is first truncated and then some zeros q_k of $\det(\mathbf{W})$ are computed numerically. These zeros yield the approximate eigenvalues.

The computation of the associated eigenfunctions is standard. At each value q_k, the system of linear equations $\mathbf{AW} = 0$ is under-determined and has infinitely many solutions. If the eigenvalue $\lambda_k = -q_k^2$ is simple, one can fix a solution by setting one of unknown coefficients, e.g., A^1_{00}, to a constant c. This results in a smaller system of *inhomogeneous* linear equations on the remaining coefficients A^j_{mn} that can be solved numerically. The corresponding eigenfunction is given by Eq. (24). The arbitrary constant c is simply a choice of the normalization of that eigenfunction. Once the eigenfunction is constructed, it can be renormalized appropriately. For eigenvalues with multiplicity $m > 1$, an eigenfunction is defined up to m free constants that can be chosen in a standard way.

E. Dirichlet-to-Neumann operator

The GMSV can be applied to investigate the spectral properties of the Dirichlet-to-Neumann operator. For a given function f on the boundary $\partial\Omega$, the Dirichlet-to-Neumann operator $\mathcal{M}_p$ associates another function $g = (\partial w/\partial \boldsymbol{n})_{|\partial\Omega}$ on that boundary, where w is the solution of the Dirichlet boundary value problem

$$(p - D\nabla^2) w = 0 \quad (\boldsymbol{x} \in \Omega), \qquad w|_{\partial\Omega} = f \qquad (26)$$

(for an exterior problem, the regularity condition $w(\boldsymbol{x}) \to 0$ as $|\boldsymbol{x}| \to \infty$ is also imposed; see[55–59] for a rigorous mathematical definition). The Dirichlet-to-Neumann operator can be used as an alternative to the Laplace operator in describing diffusion-reaction processes. In particular, the eigenvalues and eigenfunctions of $\mathcal{M}_p$ determine most diffusion-reaction characteristics, even for inhomogeneous surface reactivity[60,61].

As the boundary $\partial\Omega$ is the union of non-intersecting spheres $\partial\Omega_i$, a function f on $\partial\Omega$ can be represented by its restrictions $f_i = f|_{\partial\Omega_i}$, and Eq. (4) is the semi-analytical solution of Eq. (26), by setting $q = \sqrt{p/D}$, $a_i = 1$ and $b_i = 0$. The action of the operator $\mathcal{M}_p$ can be determined by computing the normal derivative of the solution w. In Appendix A 4, we represented the normal derivative as

$$\left(\frac{\partial w}{\partial \boldsymbol{n}}\right)\Big|_{\partial\Omega_i} = \sum_{m,n} \left(\mathbf{F}\tilde{\mathbf{W}}^{-1}\tilde{\mathbf{W}}'\right)^i_{mn} Y_{mn}(\theta_i, \phi_i), \qquad (27)$$

where the matrices $\tilde{\mathbf{W}}$ and $\tilde{\mathbf{W}}'$ are defined by explicit formulas (A41, A43), and we inverted Eq. (13) to express the coefficients $\mathbf{A}$. As a consequence, the Dirichlet-to-Neumann operator $\mathcal{M}_p$ is represented in the basis of spherical harmonics by the following matrix

$$\mathbf{M} = \tilde{\mathbf{W}}^{-1}\tilde{\mathbf{W}}'. \qquad (28)$$

In particular, the eigenvalues of this matrix coincide with the eigenvalues of $\mathcal{M}_p$, whereas its eigenvectors allow one to reconstruct the eigenfunctions of $\mathcal{M}_p$. In practice, one computes a truncated version of the matrix $\mathbf{M}$ so that its eigenvalues would approximate a number of eigenvalues of $\mathcal{M}_p$. For the exterior problem, one needs to reduce the matrices $\tilde{\mathbf{W}}$ and $\tilde{\mathbf{W}}'$ by removing the block row and block column corresponding to Ω_0 (see Appendix A 2). We recall that, in contrast to the Laplace operator, whose spectrum is continuous for the exterior problem, the spectrum of the Dirichlet-to-Neumann operator is discrete for interior and exterior perforated domains, because their boundary $\partial\Omega$ is bounded in both cases.

The above method can also be adapted to study an extension of the Dirichlet-to-Neumann to the case when some spheres Ω_i are reflecting. In fact, let I denote the set of indices of spheres $\partial\Omega_i$ that are reactive, whereas the remaining spheres with indices $\{0, 1, \ldots, N\}\backslash I$ are reflecting. Then one can define the Dirichlet-to-Neumann operator $\mathcal{M}_p^\Gamma$, acting on a function f on $\Gamma = \cup_{i\in I}\partial\Omega_i$ as $\mathcal{M}_p^\Gamma \ : \ f \to g = (\partial w/\partial \boldsymbol{n})|_\Gamma$, where w is the solution of the mixed boundary value problem:

$$(p - D\nabla^2)w = 0 \quad \text{in } \Omega, \qquad \begin{cases} w|_\Gamma = f, \\ (\partial w/\partial \boldsymbol{n})|_{\Omega\backslash\Gamma} = 0. \end{cases} \qquad (29)$$

The matrix representation of the operator $\mathcal{M}_p^\Gamma$ is still given by Eq. (28), in which the matrix $\tilde{\mathbf{W}}$ is replaced by another matrix evaluated with $a_i = 1$, $b_i = 0$ for $i \in I$ (Dirichlet condition) and $a_i = 0$, $b_i = 1$ for $i \in \{0, 1, \ldots, N\}\backslash I$ (Neumann condition), see Appendix A 2.

III. DISCUSSION

The previous section presented a concise overview of several major applications of the GMSV for the modified Helmholtz equation. In this section, we discuss its practical aspects and illustrate the use of the GMSV on several examples in the context of chemical physics.

A. First-passage properties

As the Green function $G(\boldsymbol{x}, \boldsymbol{y}; q)$ is related via Eq. (21) to the Laplace transform of the heat kernel, it determines most diffusion-reaction characteristics in the Laplace domain (see[60] for details). For instance, the Laplace transform of the probability flux density $j(\boldsymbol{s}, t|\boldsymbol{y})$ reads

$$\tilde{j}(\boldsymbol{s}, p|\boldsymbol{y}) = \int_0^\infty dt\, e^{-pt}\, j(\boldsymbol{s}, t|\boldsymbol{y}) = \left(-\frac{\partial G(\boldsymbol{x}, \boldsymbol{y}; \sqrt{p/D})}{\partial \boldsymbol{n}}\right)\Big|_{\boldsymbol{x}=\boldsymbol{s}\in\partial\Omega}. \qquad (30)$$

We recall that $j(\boldsymbol{s}, t|\boldsymbol{y})$ is the joint probability density of the reaction time and location on the partially reactive boundary $\partial\Omega$ for a particle started from a point $\boldsymbol{y} \in \Omega$. The normal derivative of the Green function was evaluated in Appendix A 4, yielding:

$$\tilde{j}(\boldsymbol{s}, p|\boldsymbol{y})\Big|_{\partial\Omega_i} = \sum_{m,n} \mathbf{J}^i_{mn}(\boldsymbol{y})\, Y_{mn}(\theta_i, \phi_i), \qquad (31)$$

where the components of the vector $\mathbf{J}$ are given by Eq. (A47), with $q = \sqrt{p/D}$.

Probability distribution of the reaction time

The integral of the joint probability density $j(\boldsymbol{s}, t|\boldsymbol{y})$ over time t yields the spread harmonic measure density on the sphere $\partial\Omega_i$[62,63]. This is a natural extension of the harmonic measure density to partially reactive traps with Robin boundary condition, which characterizes the distribution of the reaction location. As the integral of $j(\boldsymbol{s}, t|\boldsymbol{y})$ over t is equal to $\tilde{j}(\boldsymbol{s}, 0|\boldsymbol{y})$ (i.e., with $p = q = 0$), the modified Helmholtz equation is reduced to the Laplace equation. The explicit representation of the spread harmonic measure density and its properties were discussed in Ref.[31].

In turn, the integral of $j(\boldsymbol{s}, t|\boldsymbol{y})$ over the location position $\boldsymbol{s}$ yields the probability density of the reaction time:

$$H(t|\boldsymbol{y}) = \int_{\partial\Omega} d\boldsymbol{s}\, j(\boldsymbol{s}, t|\boldsymbol{y}). \qquad (32)$$

In the Laplace domain, the expansion (31) allows one to easily compute this integral due to the orthogonality of

spherical harmonics:

$$\tilde{H}(p|\boldsymbol{y}) = \int\limits_{\partial\Omega} d\boldsymbol{s}\, \tilde{j}(\boldsymbol{s}, p|\boldsymbol{y}) = \sqrt{4\pi} \sum_{i=0}^{N} R_i^2\, \mathbf{J}^i_{00}(\boldsymbol{y}), \qquad (33)$$

where the factor R_i^2 accounts for the area of the i-th ball, and the matrix elements $\mathbf{J}^i_{00}(\boldsymbol{y})$ are given in Eq. (A50). Note that each term in this sum is the probability flux onto the sphere $\partial\Omega_i$, while the dependence on $\boldsymbol{y}$ comes explicitly through the expression for $\mathbf{J}$. By definition, $\tilde{H}(p|\boldsymbol{y}) = \langle \exp(-p\mathcal{T})\rangle$ is the generating function of the moments of the reaction time $\mathcal{T}$:

$$\langle \mathcal{T}^k \rangle = (-1)^k \lim_{p\to 0} \frac{\partial^k \tilde{H}(p|\boldsymbol{y})}{\partial p^k}\,. \qquad (34)$$

One can thus determine the mean and higher-order moments of the reaction time $\mathcal{T}$. In turn, the inverse Laplace transform of Eq. (33) gives $H(t|\boldsymbol{y})$ in time domain. The integral of $H(t|\boldsymbol{y})$ from 0 to t yields the probability of reaction up to time t, whereas the integral from t to infinity is the survival probability of the particle. We conclude that the present approach opens new opportunities for studying various first-passage phenomena for an arbitrary configuration of non-overlapping partially reactive spherical traps. In other words, this approach generalizes the classical results for diffusion outside a single trap, for which one has $\mathbf{U} = 0$, and the above expression simplifies to

$$\tilde{H}(p|\boldsymbol{y}) = \frac{R_1\, e^{-\sqrt{p/D}(|\boldsymbol{y}|-R_1)}}{|\boldsymbol{y}|(a_1 + b_1(1 + R_1\sqrt{p/D}))}\,, \qquad (35)$$

where we used the Wronskian

$$i_n'(z)k_n(z) - k_n'(z)i_n(z) = \frac{1}{z^2} \qquad (36)$$

and the explicit relations $i_0(z) = \sinh(z)/z$ and $k_0(z) = e^{-z}/z$. The inverse Laplace transform of this formula yields the expression for $H(t|\boldsymbol{y})$ derived by Collins and Kimball[64]. Setting $a_1 = 1$ and $b_1 = 0$, one retrieves another classical expression for a perfectly reactive trap studied by von Smoluchowski[65]. We emphasize that for a single trap, the analysis can be pushed much further by including, e.g., the interaction potentials (see[66–68] and references therein). The more elaborate example of two concentric spheres is discussed in Appendix C.

Presence of reflecting obstacles?

How do reflecting obstacles modify the reaction time distribution? Figure 3 presents the Laplace-transformed probability density $\tilde{H}(p|0)$ of the first-exit time from the center of the ball of radius $R_0 = R$ to its boundary $\partial\Omega_0$ in presence of 35 reflecting spherical obstacles of equal radii $R_i = \rho$. In Ref.[70], we conjectured that reflecting obstacles cannot speed up the exit from the center of the ball,

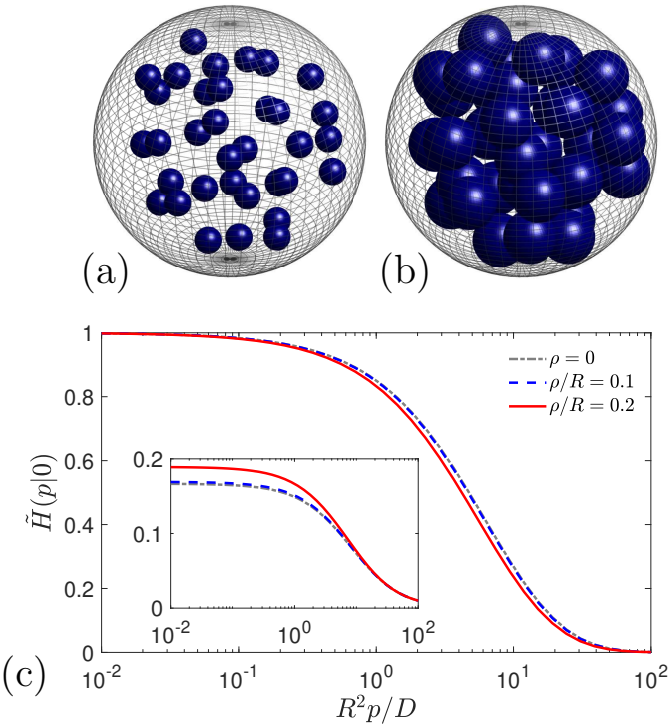

FIG. 3: **(a,b)** Two configurations of 35 reflecting spherical obstacles of radius ρ inside a larger sphere of radius R, with the same centers but distinct radii: $\rho/R = 0.1$ **(a)** and $\rho/R = 0.2$ **(b)**. **(c)** Laplace-transformed probability density $\tilde{H}(p|0)$ of the first-exit time from the center of the ball of radius R to its boundary $\partial\Omega_0$ in presence of 35 reflecting spherical obstacles. The function $\tilde{H}(p|0)$ was computed via Eq. (33), with the truncation order $n_{\max} = 2$. For comparison, the gray dash-dotted line shows the classical expression $\tilde{H}(p|0) = 1/i_0(R\sqrt{p/D})$ for an empty ball without obstacles. The inset shows the Laplace-transformed survival probability $\tilde{S}(p|0) = (1 - \tilde{H}(p|0))/p$.

i.e., $S(t|0) \geq S_0(t|0)$, where $S(t|0)$ and $S_0(t|0)$ are the survival probabilities with and without obstacles, respectively. As a consequence, their Laplace transforms satisfies the same inequality: $\tilde{S}(p|0) \geq \tilde{S}_0(p|0)$. This statement is not trivial: on one hand, reflecting obstacles hinder the motion of the diffusing particle and thus increase its first-exit time; on the other hand, the obstacles reduce the available space that might speed up the exit. According to this conjecture, the hindering effect always "wins" for diffusion from the center to the boundary of a ball, but it is not necessarily true neither for other starting points, nor for other (non-spherical) domains. This conjecture is confirmed in our numerical example, as illustrated in the inset of Fig. 3. Expectedly, small obstacles ($\rho/R = 0.1$) almost do not alter $\tilde{H}(p|0)$ and $\tilde{S}(p|0)$, the curves being barely distinguishable. Most surprisingly, even large obstacles ($\rho/R = 0.2$) that fill $35(\rho/R)^3 \approx 28\%$ of the volume, also have a very moderate effect, which is mainly visible on the inset at small p. Indeed, the ob-

stacles hinder diffusion and slightly increase the mean first-exit time $\tilde{S}(p=0|0)$, from $R^2/(6D) \approx 0.17(R^2/D)$ without obstacles, to $0.19(R^2/D)$ in the presence of obstacles. Even though this observation is realized for the particular geometric setting of spherical obstacles, one can question the role of hindering obstacles in more general configurations. A systematic study of this problem can be performed in future by using the present numerical and analytical approach. As discussed in Sec. III B, $\tilde{H}(p|0)$ can alternatively be interpreted as the stationary concentration at $\boldsymbol{y}=0$ of mortal particles whose concentration on the outer boundary is kept constant.

Presence of absorbing sinks?

With the help of the GMSV, one can refine the above analysis by considering the following first-passage time problem: for a particle started from $\boldsymbol{y}$, what is the reaction time on a given trap i in the presence of absorbing sinks that can irreversibly bind the diffusing particle? The role of such binding sites onto the protein search for targets on DNA chain was recently investigated within a simplified one-dimensional model[69]. The GMSV allows one to push this analysis further toward more elaborate geometric configurations. The related survival probability $S(t|\boldsymbol{y})$ satisfies the backward diffusion equation:

$$\frac{\partial S(t|\boldsymbol{y})}{\partial t} - D\nabla^2 S(t|\boldsymbol{y}) = 0 \quad (\boldsymbol{y}\in\Omega), \tag{37a}$$

$$\left(a_i S + b_i R_i \frac{\partial S}{\partial \boldsymbol{n}}\right)\Big|_{\partial\Omega_i} = 0, \tag{37b}$$

$$S(t|\boldsymbol{y})\big|_{\partial\Omega_j} = 1 \quad (j\neq i), \tag{37c}$$

with the initial condition $S(t=0|\boldsymbol{y})=1$. We emphasize that this probability characterizes the reaction events on the trap i; if in turn the particle binds any absorbing sink (with $j\neq i$), it survives forever, see Eq. (37c). The probability density of the reaction time is still $H(t|\boldsymbol{y}) = -\partial S(t|\boldsymbol{y})/\partial t$ but it is not normalized to 1 given that the reaction may never happen due to irreversible binding.

The Laplace transform reduces the diffusion equation (37a) to the modified Helmholtz equation. Rewriting this equation for the Laplace-transformed probability density, $\tilde{H}(p|\boldsymbol{y}) = 1 - p\tilde{S}(p|\boldsymbol{y})$, one gets

$$(p - D\nabla^2)\tilde{H}(p|\boldsymbol{y}) = 0 \quad (\boldsymbol{y}\in\Omega), \tag{38a}$$

$$\left(a_j \tilde{H} + b_j R_j \frac{\partial \tilde{H}}{\partial \boldsymbol{n}}\right)\Big|_{\partial\Omega_j} = a_j\delta_{ij} \quad (j=0,\ldots,N), \tag{38b}$$

where $a_j = 1$ and $b_j = 0$ for all $j\neq i$. As this is a specific case of the general boundary value problem considered in Sec. II A, its semi-analytical solution is accessible via the GMSV. If one is interested in finding the reaction time on a subset I of traps, the condition $a_j = 1$ and $b_j = 0$ is imposed only for $j\notin I$, and the right-hand side of Eq. (38b) becomes $a_j 1_{j\in I}$, where $1_{j\in I}$ is the boolean variable taking 1 if $j\in I$ and 0 otherwise. When $I=\{0,1,\ldots,N\}$, one retrieves the standard first-passage time problem, with a_j standing in the right-hand side for all j. Note also that some traps from the subset I can be reflecting and thus represent passive obstacles. Finally, as $\tilde{H}(0|\boldsymbol{y})$ is the integral of $H(t|\boldsymbol{y})$, it can be interpreted as the probability of reaction, also known as the splitting probability for perfectly reactive traps.

B. Stationary diffusion of mortal particles

In the case of perfectly absorbing traps ($a_i=1$, $b_i=0$), the boundary condition (38b) simply reads $\tilde{H}|_{\partial\Omega_j} = \delta_{ij}$, and the above first-passage time problem is equivalent to stationary diffusion of "mortal" particles, which move from a source on $\partial\Omega_i$ to perfect sinks on the remaining spheres $\partial\Omega_j$ and spontaneously disappear with the bulk rate p. This is a very common situation in biological and chemical diffusion-reaction processes. Among typical examples, one can mention: spermatozoa moving in an aggressive medium toward an egg cell; bacteria or viruses that can be neutralized by the immune system; cells or animals searching for food and starving to death; proteins or RNA molecules which can disassemble and be recycled within the cell; fluorescent proteins diffusing toward receptors and spontaneously loosing their signal and thus disappearing from view in single-particle tracking experiments; excited nuclei loosing their magnetization due to relaxation processes in nuclear magnetic resonance experiments; diffusing radioactive nuclei that may disintegrate on their way from the nuclear reactor core; more generally, molecules that can be irreversibly bound to bulk constituent or be chemically transformed on their way to catalytic sites[70–74]. For instance, setting a constant concentration c_0 on the outer sphere $\partial\Omega_0$ and zero concentration on the inner spheres $\partial\Omega_j$ describes the diffusive flux of particles toward perfect sinks. Alternatively, one can impose a constant flux on the outer sphere to model particles constantly coming onto $\partial\Omega_0$ from the exterior space. Similarly, any set of inner balls can play the role of a source. In turn, setting Neumann condition on some inner spheres switches them to inert obstacles, whereas Robin condition describes an intermediate behavior. The diffusive flux onto the trap Ω_j is then obtained from Eq. (27):

$$J_j = \int\limits_{\partial\Omega_j} d\boldsymbol{s}\, \left(-Dc_0 \frac{\partial \tilde{H}(p|\boldsymbol{y})}{\partial \boldsymbol{n}}\right)\Big|_{\boldsymbol{y}=\boldsymbol{s}\in\partial\Omega_j}$$
$$= -\sqrt{4\pi} c_0 D R_j^2 \big(\mathbf{F}\mathbf{M}^\dagger\big)^j_{00}, \tag{39}$$

where the matrix $\mathbf{M}$ is defined by Eq. (28), and we used the orthogonality of spherical harmonics. Here, the components of the vector $\mathbf{F}$ from Eq. (12) describe whether the i-th ball is source or sink. For instance, if there is a single source located on the sphere $\partial\Omega_i$, then $f_j(\boldsymbol{s}) = \delta_{ij}$

and thus $F^j_{mn} = \delta_{ij}\delta_{n0}\delta_{m0}\sqrt{4\pi}$ so that

$$J_j = -4\pi D c_0 R_j^2 (\mathbf{M})^{ji}_{00,00}. \tag{40}$$

Expectedly, the flux is positive on traps and negative on the source. When there is a subset of sources, then this expression is summed over i corresponding to sources. Note that all balls can be treated as sources, in which case particles disappear only due to the bulk rate p.

As an example, let us consider two concentric spheres and assign the outer sphere Ω_0 to be a source and the inner sphere Ω_1 to be a sink. In this elementary setting, one gets an explicit solution

$$w(\boldsymbol{x};q) = c_0 \frac{i_0(q|\boldsymbol{x}|)k_0(qR_1) - k_0(q|\boldsymbol{x}|)i_0(qR_1)}{i_0(qR_0)k_0(qR_1) - k_0(qR_0)i_0(qR_1)}, \tag{41}$$

$$J_1 = \frac{4\pi c_0 D q R_0 R_1}{\sinh(q(R_0 - R_1))}, \tag{42}$$

with $q = \sqrt{p/D}$. In the limit $p \to 0$ and $R_0 \to \infty$, one retrieves the Smoluchowski formula for the steady-state reaction rate of a ball of radius R_1: $J_1 = 4\pi c_0 D R_1$.

Reaction rate

On the other hand, the integral of $\tilde{j}(\boldsymbol{s}, p|\boldsymbol{y})$ from Eq. (31) yields the probability flux onto the sphere $\partial\Omega_i$ from a point source at $\boldsymbol{y}$. If there is a constant bulk uptake (with concentration c_0), the diffusive uptake onto the trap $\partial\Omega_i$ is given by

$$\overline{J}_i(p) = c_0 \int_\Omega d\boldsymbol{y} \int_{\partial\Omega_i} d\boldsymbol{s}\, \tilde{j}(\boldsymbol{s}, p|\boldsymbol{y})\big|_{\partial\Omega_i} = \sqrt{4\pi} c_0 R_i^2 \overline{\mathbf{J}}^i_{00}, \tag{43}$$

where $\overline{\mathbf{J}}$ is the vector with components $\overline{J}^i_{mn}$ given by Eq. (A54) after an explicit integration of the elements of the vector $\mathbf{J}$ over the starting point $\boldsymbol{y}$. This is the amount of molecules (e.g., in mole) that have not disappeared in the bulk and come to the trap Ω_i. This quantity can also be interpreted as the Laplace transform of the time-dependent reaction rate $J_i(t)$ for the i-th trap, if the molecules were initially distributed uniformly in the domain (with concentration c_0). The Laplace-transformed total reaction rate is then obtained by summing these diffusive fluxes:

$$\tilde{J}(p) = \sum_{i=0}^{N} \overline{J}_i(p). \tag{44}$$

For the exterior problem, the term $i = 0$ corresponding to the outer boundary is removed. In this case, $\tilde{J}(p) \propto 1/p$ as $p \to 0$, and the proportionality coefficient is the steady-state reaction rate in the long-time limit.

For instance, for the exterior problem for a single sphere, one easily gets from Eq. (A54) that $\overline{\mathbf{J}}^i_{00} = \sqrt{4\pi} k_1(qR_1)/(qk_0(qR_1))$, from which

$$\tilde{J}_{\rm sm}(p) \equiv \overline{J}_1(p) = 4\pi c_0 D R_1 \left(\frac{1}{p} + \frac{R_1}{\sqrt{pD}}\right). \tag{45}$$

This is the Laplace transform of the classical Smoluchowski rate on the perfectly reactive sphere[65]:

$$J_{\rm sm}(t) = 4\pi c_0 D R_1 \big(1 + R_1/\sqrt{\pi D t}\big). \tag{46}$$

We illustrate the effect of diffusion screening between traps onto the reaction rate by considering several configurations of 6 identical perfect traps of radius $\rho = 1/6$ located along the axes at distance L from the origin (Fig. 4(a)). Figure 4(b) shows the Laplace-transformed reaction rate $\tilde{J}(p)$, which is normalized by the above Smoluchowski rate $\tilde{J}_{\rm sm}(p)$ for a single spherical trap of radius $R_1 = 6\rho = 1$. In the limit of $p \to 0$ (no bulk reaction), the curves tend to constants, indicating the common behavior $\tilde{J}(p) \propto 1/p$. As L increases, the traps become more distant and compete less for diffusing particles so that the reaction rate increases. Moreover, the particular choice $\rho = R_1/6$ ensures that the ratio $\tilde{J}(0)/\tilde{J}_{\rm sm}(0)$ approaches 1 as $L \to \infty$: 6 very distant balls of radius ρ trap the particles as efficiently as a single trap of radius 6ρ. This is a reminiscent feature of diffusion-limited reactions and of the Smoluchowski rate, which is proportional to R_1 in the limit $p \to 0$.

In contrast, the opposite limit $p \to \infty$ corresponds to the short-time behavior of the reaction rate. As particles diffuse on average over a distance $\sqrt{Dt}$, the 6 balls trap first the particles in their close vicinity and thus do not compete. As a consequence, the total reaction rate does not depend on the distance L (if L exceeds $\sqrt{Dt}$), as clearly seen on Fig. 4. Moreover, in this limit, the second term dominates in Eq. (45), and the reaction rate is proportional to the squared radius that explains 6 times smaller limit of $\tilde{J}(p)/\tilde{J}_{\rm sm}(p)$ as $p \to \infty$.

Figure 4(c) illustrates these results in time domain by showing the total flux $J(t)$, which is obtained via a numerical Laplace transform inversion of $\tilde{J}(p)$ and then normalized by $J_{\rm sm}(t)$ from Eq. (46). At long times (corresponding to $p \to 0$), the total flux reaches its steady-state limit. At short times (corresponding to $p \to \infty$), all curves reach the same level 1/6, which is the ratio between the total surface area of 6 balls of radius $\rho = 1/6$ and the total surface area of a single ball of radius $R_1 = 6\rho$.

Finally, we note that the reaction rates on Fig. 4 were obtained by truncating matrices up to the order $n_{\max} = 2$. As we dealt with matrices of size $6(2+1)^2 \times 6(2+1)^2 = 54 \times 54$, all curves were obtained within less than a second on a standard laptop. Remarkably, the use of the lowest truncation order $n_{\max} = 0$ yielded very accurate results (shown by symbols) when the traps are well separated (i.e., $L \gg \rho$). But even for close traps ($L = 0.25$), the error was not significant. From our experience, this is a common situation for exterior problems. For interior problems, the quality of the monopole approximation is usually lower.

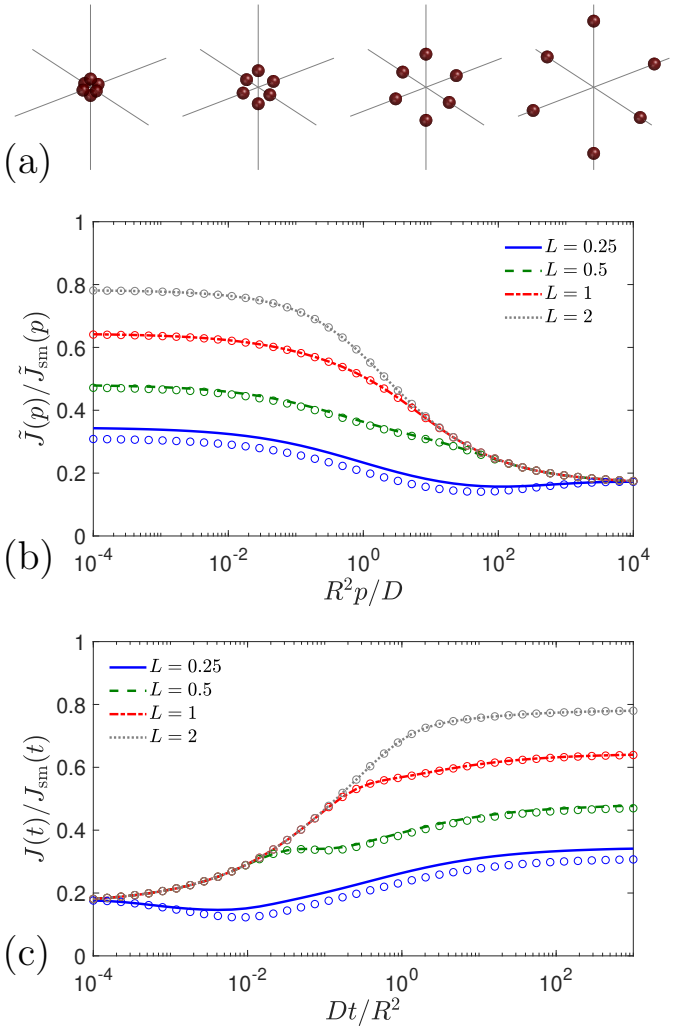

FIG. 4: **(a)** Four configurations of 6 perfect sinks of radius $\rho = 1/6$ located on the axes at distance L from the origin, with $L = 0.25, 0.5, 1, 2$. **(b)** Laplace-transformed total flux $\tilde{J}(p)$ onto 6 sinks, normalized by $\tilde{J}_{\rm sm}(p)$ from Eq. (45) for the unit sphere ($R = 1$). Solid lines show $\tilde{J}(p)$ computed via Eq. (44) with the truncation order $n_{\max} = 2$; symbols show the results obtained with $n_{\max} = 0$ (monopole approximation). **(c)** The corresponding total fluxes $J(t)$, obtained via the numerical inversion of the Laplace transform by the Talbot algorithm, which is normalized by $J_{\rm sm}(t)$ from Eq. (46) for the unit sphere.

C. Advantages and limitations

As discussed in Sec. I, different numerical methods have been applied for solving boundary value problems for the modified Helmholtz equation. In contrast to these conventional methods, the GMSV relies on the local spherical symmetries of perforated domains made of non-overlapping balls. In other words, the solution $w(\boldsymbol{x}; q)$ is decomposed on the basis functions $\psi^{\pm}_{mn}$, which are written in local spherical coordinates and thus respect *locally* the symmetry of the corresponding trap. As a consequence, such decompositions can often be truncated after few terms and still yield accurate results. An important advantage of the method is that the dependence on $\boldsymbol{x}$ is analytical and explicit: once the coefficients are found numerically, the solution and its spatial derivatives can be easily calculated (and refined) at any set of points. Moreover, integrals of the solution over spherical boundaries or balls can be found analytically with the help of re-expansions (see Appendix A 5). The meshless character of the GMSV makes it an alternative to the method of fundamental solutions (see[75] and references therein).

Another important advantage of this method is the possibility of solving *exterior* problems (when $\Omega_0 = \mathbb{R}^3$), which are particularly difficult from the numerical point of view. In fact, a practical implementation of standard discretization schemes such as finite difference or finite elements methods would require introducing an artificial outer boundary to deal with a finite volume. An outer boundary is also needed in Monte Carlo simulations due to the transient character of the three-dimensional Brownian motion. In contrast, the present approach does not require any outer boundary because the solution is constructed on the appropriate basis functions that vanish at infinity. Exterior problems are actually simpler than interior ones, as there is no need to impose boundary condition on the outer boundary $\partial\Omega_0$. In this light, the present approach is a rather unique numerical tool to deal with various exterior boundary value problems.

Finally, the GMSV opens access to such fundamental entities as the Green function $G(\boldsymbol{x}, \boldsymbol{y}; q)$, the Laplace operator ∇^2, and the Dirichlet-to-Neumann operator $\mathcal{M}_p$. For instance, the eigenbasis of the Laplace operator yields spectral decompositions of solutions of diffusion and wave equations. In turn, the eigenbasis of the Dirichlet-to-Neumann operator allows one to deal with inhomogeneous reactivity on traps[60]. The spectral properties of both operators in perforated domains will be investigated in a separate paper.

As any numerical technique, the proposed method has its limitations from the numerical point of view. For the truncation order $n_{\max}$, there are $(n_{\max}+1)^2$ basis functions $\psi^{\pm}_{mn}$ for each ball so that the total number of unknown coefficients A^i_{mn} for a domain with N traps is $N(n_{\max}+1)^2$ for the exterior problem and $(N+1)(n_{\max}+1)^2$ for the interior problem. Their numerical computation involves the construction and inversion of the matrix $\mathbf{W}$ of size $N(n_{\max}+1)^2 \times N(n_{\max}+1)^2$. To speed up the construction of the matrix elements, we adapted recurrence relations for addition theorems from Ref.[76], see Appendix B 2. However, the direct inversion of $\mathbf{W}$ becomes very time-consuming when the number of traps N and/or the truncation order $n_{\max}$ grow. As some re-expansion formulas have a limited validity range (see Appendix A 2), their truncations should include more basis functions when the balls are close to each other. In other words, computations for dense packings of balls need larger $n_{\max}$. In such cases, one has

to resort to iterative methods (see discussion in Ref.[31]). Significant numerical improvements of this approach can be achieved by using fast multipole methods[39,40,50,77–81]. Note also that the size of the matrices is reduced to $N(n_{\max}+1)\times N(n_{\max}+1)$ in the case of axiosymmetrical problems by using special forms of re-expansion theorems[47]. Another drawback of the method is that the parameter q enters in all matrix elements that requires recomputing these matrices for each value of q. This is inconvenient for a numerical computation of the inverse Laplace transform of a solution of the modified Helmholtz equation in order to get back to time domain (see discussion in Appendix B 3 and in Ref.[48]). In turn, one can still analyze the short-time and long-time asymptotic behaviors by considering the large-q and small-q limits, respectively.

D. Extensions

The GMSV can be further extended. For instance, we assumed that a_i and b_i are nonnegative constants. This assumption can be relaxed by considering a_i and b_i as continuous nonnegative functions on each sphere $\partial\Omega_i$. The overall method is still applicable, even though its practical implementation is more elaborate. In fact, the matrix elements $W^{j,i}_{mn,kl}$ and F^{j}_{mn} will involve the scalar products of the form $(Y_{mn}, a_i Y_{kl})_{L_2(\partial\Omega_i)}$ and $(Y_{mn}, b_i Y_{kl})_{L_2(\partial\Omega_i)}$ that need to be computed. Even so such computations are rather standard (see, e.g.,[60]), we do not discuss this general setting in detail. One can also consider other canonical domains (e.g., cylinders) for which re-expansion theorems are available[82].

Another direction for extensions consists in considering more sophisticated kinetics on the boundary. The Robin boundary condition employed in the present work describes irreversible binding/reaction on an impermeable boundary (e.g., of a solid catalyst). In many biological and technological applications, the boundary is a semi-permeable membrane that separates liquid and/or gaseous phases (e.g., intracellular and extracellular compartments). To describe diffusion in both phases, one can introduce two Green functions (satisfying the modified Helmholtz equation in each phase) and couple them via two exchange boundary conditions. Expanding the Green function over basis functions in each phase, one can establish the system of linear algebraic equations on their coefficients, in a very similar way as done in Sec. II A, see Ref.[31] for a detailed implementation in the case of the Laplace equation. Yet another option is to allow for reversible binding to the balls. In the Laplace domain, the reversible binding can be implemented by replacing the constant reactivity by an effective p-dependent reactivity[83–88]. In other words, the coefficients a_i become p-dependent but the whole method remains applicable without any change. Note that each trap can be characterized by its own dissociation rate. This extension allows one to investigate the role of immobile buffering molecules in signalling processes, DNA search processes, and gene regulations, as well as many other chemical reactions (see[69,89–91] and references therein).

IV. CONCLUSION

The GMSV was broadly employed for solving boundary value problems for the Laplace and ordinary Helmholtz equations in different disciplines ranging from electrostatics to hydrodynamics and scattering theory. Quite surprisingly, applications of this powerful method to the modified Helmholtz equation, which plays the crucial role for describing diffusion-reaction processes in chemical physics, are much less developed. In the present paper, we described a general analytical and numerical framework for solving such problems in perforated domains made of non-overlapping balls. In particular, we provided a semi-analytical solution $w(\boldsymbol{x};q)$, in which the dependence on the point $\boldsymbol{x}$ enters *analytically* through explicitly known basis functions $\psi^{\pm}_{mn}$, while their coefficients are obtained *numerically* by truncating and solving the established system of linear algebraic equations. The high numerical efficiency of this approach relies on exploiting the local symmetries of the spherical traps and using the most natural basis functions.

We applied this method to derive a semi-analytical representation of the Green function that determines various characteristics of non-stationary diffusion among partially reactive traps such as the probability flux density, the reaction rate, the survival probability, and the associated probability density of the reaction time. We also showed how this method can be adapted to obtain the eigenvalues and eigenfunctions of the Laplace operator and of the Dirichlet-to-Neumann operator. These operators play an important role in mathematical physics and have been applied in a variety of disciplines, including chemical physics.

We described several applications of this technique such as the first-passage properties and stationary diffusion of mortal particles. In particular, we checked the conjecture that reflecting obstacles cannot speed up the exit from the center of a ball. Interestingly, the presence of even large obstacles had a minor effect on the distribution of the first-exit time. We also discussed how the mutual distance between absorbing traps affects the reaction rate. This discussion brings complementary insights onto the role of diffusion screening (or interaction) onto the reaction rate, which was thoroughly investigated in the steady-state limit ($t\to\infty$) but remains less known in the time-dependent regime. More generally, the developed framework provides a solid theoretical ground and efficient numerical tool for studying diffusion-controlled reactions in various media that can be modeled by spherical traps and obstacles.

Acknowledgments

The author thanks Prof. S. D. Traytak for fruitful discussions.

Data Availability Statement

The data that support the findings of this study are available from the corresponding author upon reasonable request.

Appendix A: Technical derivations

1. Re-expansion theorems

The efficiency of the GMSV relies on re-expansion (or addition) theorems that allow one to represent the basis functions $\psi^{\pm}_{mn}(qr_j,\theta_j,\phi_j)$, written in the local spherical coordinates (r_j,θ_j,ϕ_j) associated with the ball Ω_j, in terms of the basis functions $\psi^{\pm}_{mn}(qr_i,\theta_i,\phi_i)$ in the local spherical coordinates (r_i,θ_i,ϕ_i) associated with the ball Ω_i. We first recall three re-expansion theorems for the ordinary Helmholtz equation and then adapt them to the modified Helmholtz equation.

Let us denote by $\boldsymbol{L}_{ij}=\boldsymbol{x}_i-\boldsymbol{x}_j$ the vector connecting the centers of balls j and i, and $(L_{ij},\Theta_{ij},\Phi_{ij})$ are the spherical coordinates of the vector $\boldsymbol{L}_{ij}$ (Fig. 5):

$$\begin{aligned} x_i &= x_j + L_{ij}\sin\Theta_{ij}\cos\Phi_{ij},\\ y_i &= y_j + L_{ij}\sin\Theta_{ij}\sin\Phi_{ij},\\ z_i &= z_j + L_{ij}\cos\Theta_{ij}. \end{aligned} \tag{A1}$$

For the basis functions $\tilde{\psi}^{\pm}_{mn}$ of the ordinary Helmholtz equation (22), three translational re-expansion theorems are[49,50,82,92]:

(i) regular-regular (RR) addition theorem:

$$\tilde{\psi}^{+}_{mn}(qr_j,\theta_j,\phi_j)=\sum_{k,l}\tilde{U}^{(+j,+i)}_{mn,kl}\,\tilde{\psi}^{+}_{kl}(qr_i,\theta_i,\phi_i), \tag{A2}$$

where the matrix elements of the translation operator are

$$\tilde{U}^{(+j,+i)}_{mn,kl}=\sum_{\nu=|l-n|}^{l+n} i^{\nu+l-n}\,b^{\nu}_{nmlk}\,\tilde{\psi}^{+}_{(m-k)\nu}(qL_{ij},\Theta_{ij},\Phi_{ij}), \tag{A3}$$

in which

$$\begin{aligned} b^{\nu}_{nmlk} &= (-1)^k\sqrt{4\pi(2l+1)(2n+1)/(2\nu+1)}\\ &\times\langle n,l,0,0|n,l,\nu,0\rangle\,\langle n,l,m,-k|n,l,\nu,m-k\rangle, \end{aligned} \tag{A4}$$

with $\langle j_1,j_2,m_1,m_2|j_1,j_2,j,m\rangle$ being the Clebsch-Gordan coefficients (see Ref.[93], Section 27.9);

(ii) irregular-regular (IR) addition theorem:

$$\tilde{\psi}^{-}_{mn}(qr_j,\theta_j,\phi_j)=\sum_{k,l}\tilde{U}^{(-j,+i)}_{mn,kl}\,\tilde{\psi}^{+}_{kl}(qr_i,\theta_i,\phi_i) \tag{A5}$$

(for $r_i<L_{ij}$), where

$$\tilde{U}^{(-j,+i)}_{mn,kl}=\sum_{\nu=|l-n|}^{l+n} i^{\nu+l-n}b^{\nu}_{nmlk}\,\tilde{\psi}^{-}_{(m-k)\nu}(qL_{ij},\Theta_{ij},\Phi_{ij}); \tag{A6}$$

(iii) irregular-irregular (II) addition theorem:

$$\tilde{\psi}^{-}_{mn}(qr_j,\theta_j,\phi_j)=\sum_{l,k}\tilde{U}^{(-j,-i)}_{mn,kl}\,\tilde{\psi}^{-}_{kl}(qr_i,\theta_i,\phi_i) \tag{A7}$$

(for $r_i>L_{ij}$), where

$$\tilde{U}^{(-j,-i)}_{mn,kl}=\sum_{\nu=|l-n|}^{l+n} i^{\nu+l-n}b^{l}_{nm\nu(m-k)}\tilde{\psi}^{+}_{(m-k)\nu}(qL_{ij},\Theta_{ij},\Phi_{ij}). \tag{A8}$$

We recall that the basis functions for the ordinary Helmholtz equation are

$$\tilde{\psi}^{+}_{mn}(qr_i,\theta_i,\phi_i)=j_n(qr_i)\,Y_{mn}(\theta_i,\phi_i), \tag{A9a}$$

$$\tilde{\psi}^{-}_{mn}(qr_i,\theta_i,\phi_i)=h^{(1)}_n(qr_i)\,Y_{mn}(\theta_i,\phi_i), \tag{A9b}$$

where $j_n(z)=\sqrt{\pi/(2z)}\,J_{n+1/2}(z)$ and $h^{(1)}_n(z)=\sqrt{\pi/(2z)}\,H^{(1)}_{n+1/2}(z)$ are the spherical Bessel and Hankel functions of the first kind (note that $h^{(1)}_n(z)=j_n(z)+iy_n(z)$).

For convenience, the first sign in the superscript of the matrix elements $\tilde{U}^{(\pm j,\pm i)}_{mn,kl}$ denotes the type of the basis function $\tilde{\psi}^{\pm}_{mn}(qr_j,\theta_j,\phi_j)$ to be expanded (+ for regular and − for irregular one), whereas the second sign refers to the type of the basis functions $\tilde{\psi}^{\pm}_{kl}(qr_i,\theta_i,\phi_i)$ over which the expansion is provided. While the first addition theorem holds for any values of r_i and r_j, the second and the third ones are applicable for $r_i<L_{ij}$ and $r_i>L_{ij}$, respectively (see Fig. 5). In the above expressions, we used tilde to outline that the involved basis functions and the matrix elements correspond to the ordinary Helmholtz equation.

Replacing q by iq and using the relations

$$j_n(iz)=i^n i_n(z),\qquad h^{(1)}_n(iz)=-i^{-n}k_n(z), \tag{A10}$$

one gets three translational re-expansion (or addition) theorems for the modified Helmholtz equation (Fig. 5):

(i) regular-regular (RR) addition theorem:

$$\psi^{+}_{mn}(qr_j,\theta_j,\phi_j)=\sum_{k,l}U^{(+j,+i)}_{mn,kl}\,\psi^{+}_{kl}(qr_i,\theta_i,\phi_i), \tag{A11}$$

with

$$U^{(+j,+i)}_{mn,kl}=\sum_{\nu=|l-n|}^{l+n}(-1)^{\nu+n+l}\,b^{\nu}_{nmlk}\,\psi^{+}_{(m-k)\nu}(qL_{ij},\Theta_{ij},\Phi_{ij}). \tag{A12}$$

(ii) irregular-regular (IR) addition theorem:

$$\psi^{-}_{mn}(qr_j,\theta_j,\phi_j)=\sum_{k,l}U^{(-j,+i)}_{mn,kl}\,\psi^{+}_{kl}(qr_i,\theta_i,\phi_i) \tag{A13}$$

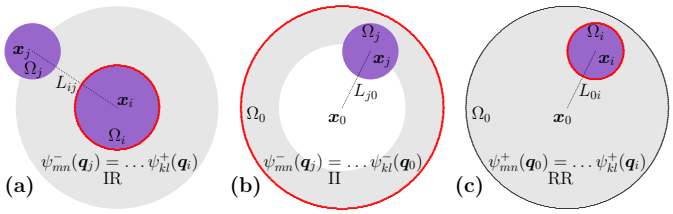

FIG. 5: Three translational re-expansion theorems that we use to decompose any basis function $\psi^{\pm}_{mn}(\boldsymbol{q}_j) = \psi^{\pm}_{mn}(qr_j,\theta_j,\phi_j)$ in the local spherical coordinates (r_j,θ_j,ϕ_j) centered at $\boldsymbol{x}_j$, on the basis functions $\psi^{\pm}_{kl}(qr_i,\theta_i,\phi_i)$ in the local spherical coordinates (r_i,θ_i,ϕ_i) centered at $\boldsymbol{x}_i$. These decompositions help us to impose the boundary condition on $\partial\Omega_i$ (shown by red circle). **(a)** The basis function $\psi^{-}_{mn}(\boldsymbol{q}_j)$ outside the ball Ω_j can be decomposed on regular functions $\psi^{+}_{kl}(\boldsymbol{q}_i)$ via the IR theorem (A13), which is valid in the shadowed (gray) region, in particular, on $\partial\Omega_i$. **(b)** In turn, to impose the boundary condition on the outer boundary $\partial\Omega_0$, the basis function $\psi^{-}_{mn}(\boldsymbol{q}_j)$ outside the ball Ω_j is decomposed on irregular functions $\psi^{-}_{kl}(\boldsymbol{q}_0)$ via the II theorem (A15), which is valid in the shadowed region, in particular, on $\partial\Omega_0$. **(c)** The basis function $\psi^{+}_{mn}(\boldsymbol{q}_0)$ inside the ball Ω_0 is decomposed on regular functions $\psi^{+}_{kl}(\boldsymbol{q}_i)$ via the RR theorem (A11), which is valid anywhere, in particular, on $\partial\Omega_i$.

(for $r_i < L_{ij}$), where

$$U^{(-j,+i)}_{mn,kl} = \sum_{\nu=|l-n|}^{l+n} (-1)^l b^{\nu}_{nmlk}\, \psi^{-}_{(m-k)\nu}(qL_{ij},\Theta_{ij},\Phi_{ij}). \tag{A14}$$

(iii) irregular-irregular (II) addition theorem:

$$\psi^{-}_{mn}(qr_j,\theta_j,\phi_j) = \sum_{l,k} U^{(-j,-i)}_{mn,kl}\, \psi^{-}_{kl}(qr_i,\theta_i,\phi_i) \tag{A15}$$

(for $r_i > L_{ij}$), where

$$U^{(-j,-i)}_{mn,kl} = \sum_{\nu=|l-n|}^{l+n} (-1)^{\nu} b^{l}_{nm\nu(m-k)}\, \psi^{+}_{(m-k)\nu}(qL_{ij},\Theta_{ij},\Phi_{ij}). \tag{A16}$$

Importantly, all the matrix elements can be found from recurrence relations that considerably speed up their computation (see Appendix B 2).

2. Matrix elements $W^{j,i}_{mn,kl}$

In this Appendix, we derive the explicit formulas for the matrix elements $W^{j,i}_{mn,kl}$ defined in Eq. (11). Even though one could in principle compute these elements by numerical integration, the derived exact explicit expressions significantly improve the speed and accuracy of the semi-analytical solution.

The matrix elements are particularly simple for $i = j$ because the basis solution $\psi^{\pm}_{mn}(qr_i,\theta_i,\phi_i)$ is written in the local spherical coordinates associated to the boundary $\partial\Omega_i$. For $i = 1,2,\ldots,N$, one has

$$\left(a_i + b_i R_i \frac{\partial}{\partial \boldsymbol{n}}\right) \psi^{-}_{mn}(qr_i,\theta_i,\phi_i)\Big|_{\partial\Omega_i} = \Big(a_i k_n(qR_i) - b_i R_i\, qk'_n(qR_i)\Big) Y_{mn}(\theta_i,\phi_i),$$

where prime denotes the derivative with respect to the argument, and the sign minus appeared from the orientation of the normal derivative: $\partial/\partial\boldsymbol{n} = -\partial/\partial r_i$. The scalar product with Y_{kl} yields

$$W^{i,i}_{mn,kl} = \delta_{nl}\delta_{mk}\big(a_i k_n(qR_i) - b_i R_i\, qk'_n(qR_i)\big), \tag{A17}$$

due to the orthonormality of the spherical harmonics. Similarly, one gets for the outer boundary ($i = j = 0$):

$$W^{0,0}_{mn,kl} = \delta_{nl}\delta_{mk}\big(a_0 i_n(qR_0) + b_0 R_0\, qi'_n(qR_0)\big). \tag{A18}$$

The major difficulty consists in computing the matrix elements $W^{j,i}_{mn,kl}$ for $i \neq j$ as one needs to re-expand the basis functions $\psi^{\pm}_{mn}(qr_j,\theta_j,\phi_j)$ in terms of the basis functions $\psi^{\pm}_{mn}(qr_i,\theta_i,\phi_i)$ with the aid of the re-expansion theorems (Sec. A 1). We start with the case $i,j = 1,2,\ldots,N$, for which the irregular-regular addition theorem is applied:

$$\begin{aligned}
&\left(a_i + b_i R_i \frac{\partial}{\partial \boldsymbol{n}}\right) \psi^{-}_{mn}(qr_j,\theta_j,\phi_j)\Big|_{\partial\Omega_i} \\
&= \sum_{k,l} U^{(-j,+i)}_{mn,kl} \left(a_i + b_i R_i \frac{\partial}{\partial \boldsymbol{n}}\right) \psi^{+}_{kl}(qr_i,\theta_i,\phi_i)\Big|_{\partial\Omega_i} \\
&= \sum_{k,l} U^{(-j,+i)}_{mn,kl} \Big(a_i i_l(qR_i) - b_i R_i\, qi'_l(qR_i)\Big) Y_{kl}(\theta_i,\phi_i).
\end{aligned}$$

The scalar product of this expression with Y_{kl} yields

$$W^{j,i}_{mn,kl} = U^{(-j,+i)}_{mn,kl}\big(a_i i_l(qR_i) - b_i R_i\, qi'_l(qR_i)\big). \tag{A19}$$

When $i = 0$ and $j = 1,2,\ldots,N$, one uses the irregular-irregular addition theorem:

$$\begin{aligned}
&\left(a_0 + b_0 R_0 \frac{\partial}{\partial \boldsymbol{n}}\right) \psi^{-}_{mn}(qr_j,\theta_j,\phi_j)\Big|_{\partial\Omega_0} \\
&= \sum_{k,l} U^{(-j,-0)}_{mn,kl} \left(a_0 + b_0 R_0 \frac{\partial}{\partial \boldsymbol{n}}\right) \psi^{-}_{kl}(qr_0,\theta_0,\phi_0)\Big|_{\partial\Omega_0} \\
&= \sum_{k,l} U^{(-j,-0)}_{mn,kl} \Big(a_0 k_l(qR_0) + b_0 R_0\, qk'_l(qR_0)\Big) Y_{kl}(\theta_0,\phi_0),
\end{aligned}$$

from which

$$W^{j,0}_{mn,kl} = U^{(-j,-0)}_{mn,kl}\big(a_0 k_l(qR_0) + b_0 R_0\, qk'_l(qR_0)\big). \tag{A20}$$

Finally, when $i = 1,2,\ldots,N$ and $j = 0$, one uses the

regular-regular addition theorem:

$$\begin{aligned}&\left(a_i + b_i R_i \frac{\partial}{\partial \boldsymbol{n}}\right) \psi^+_{mn}(qr_0, \theta_0, \phi_0)\Big|_{\partial\Omega_i} \\ &= \sum_{k,l} U^{(+0,+i)}_{mn,kl} \left(a_i + b_i R_i \frac{\partial}{\partial \boldsymbol{n}}\right) \psi^+_{kl}(qr_i, \theta_i, \phi_i)\Big|_{\partial\Omega_i} \\ &= \sum_{k,l} U^{(+0,+i)}_{mn,kl} \Big(a_i i_l(qR_i) - b_i R_i\, q i'_l(qR_i)\Big) Y_{kl}(\theta_i, \phi_i),\end{aligned}$$

from which

$$W^{0,i}_{mn,kl} = U^{(+0,+i)}_{mn,kl} \big(a_i i_l(qR_i) - b_i R_i\, q i'_l(qR_i)\big). \quad \text{(A21)}$$

In summary, the matrix $\mathbf{W}$ is formed by $(N+1)\times(N+1)$ blocks corresponding to indices $i, j = 0, 1, \ldots, N$. It is convenient to represent this matrix as

$$\mathbf{W} = \mathbf{q} + \mathbf{U}\mathbf{p}, \quad \text{(A22)}$$

with

$$\mathbf{U} = \begin{pmatrix} \mathbf{0} & \mathbf{U}^{(+0,+1)} & \mathbf{U}^{(+0,+2)} & \ldots & \mathbf{U}^{(+0,+N)} \\ \mathbf{U}^{(-1,-0)} & \mathbf{0} & \mathbf{U}^{(-1,+2)} & \ldots & \mathbf{U}^{(-1,+N)} \\ \mathbf{U}^{(-2,-0)} & \mathbf{U}^{(-2,+1)} & \mathbf{0} & \ldots & \mathbf{U}^{(-2,+N)} \\ \ldots & \ldots & \ldots & \ldots & \ldots \\ \mathbf{U}^{(-N,-0)} & \mathbf{U}^{(-N,+1)} & \mathbf{U}^{(-N,+2)} & \ldots & \mathbf{0} \end{pmatrix}, \quad \text{(A23)}$$

where the block matrices $\mathbf{U}^{(\pm j,\pm i)}$ are formed by the elements $U^{(\pm j,\pm i)}_{mn,kl}$ given above, and $\mathbf{p}$ and $\mathbf{q}$ are block-diagonal matrices with the elements

$$(\mathbf{p})^{ij}_{mn,kl} = a_i (\tilde{\mathbf{p}})^{ij}_{mn,kl} + b_i R_i (\tilde{\mathbf{p}}')^{ij}_{mn,kl}, \quad \text{(A24a)}$$

$$(\mathbf{q})^{ij}_{mn,kl} = a_i (\tilde{\mathbf{q}})^{ij}_{mn,kl} + b_i R_i (\tilde{\mathbf{q}}')^{ij}_{mn,kl}, \quad \text{(A24b)}$$

with

$$(\tilde{\mathbf{p}})^{ij}_{mn,kl} = \delta_{ij}\delta_{nl}\delta_{mk} \begin{cases} k_n(qR_0) & (i=0), \\ i_n(qR_i) & (i>0), \end{cases} \quad \text{(A25a)}$$

$$(\tilde{\mathbf{p}}')^{ij}_{mn,kl} = \delta_{ij}\delta_{nl}\delta_{mk} \begin{cases} qk'_n(qR_0) & (i=0), \\ -qi'_n(qR_i) & (i>0), \end{cases} \quad \text{(A25b)}$$

$$(\tilde{\mathbf{q}})^{ij}_{mn,kl} = \delta_{ij}\delta_{nl}\delta_{mk} \begin{cases} i_n(qR_0) & (i=0), \\ k_n(qR_i) & (i>0), \end{cases} \quad \text{(A25c)}$$

$$(\tilde{\mathbf{q}}')^{ij}_{mn,kl} = \delta_{ij}\delta_{nl}\delta_{mk} \begin{cases} qi'_n(qR_0) & (i=0), \\ -qk'_n(qR_i) & (i>0). \end{cases} \quad \text{(A25d)}$$

The first block row and the first block column of the matrix $\mathbf{U}$ are different from the other blocks as they are related to the outer boundary $\partial\Omega_0$. For the exterior problem, all $A^0_{mn} \equiv 0$ and thus the matrices $\mathbf{U}$ and $\mathbf{W}$ are reduced by removing the first block row and block column.

We can thus combine the above relations in a single expression:

$$\left(a_i + b_i R_i \frac{\partial}{\partial \boldsymbol{n}}\right) \psi^{\epsilon_j}_{mn}(qr_j, \theta_j, \phi_j)\Big|_{\partial\Omega_i} = \sum_{k,l} (\mathbf{q} + \mathbf{U}\mathbf{p})^{ji}_{mn,kl}\, Y_{kl}(\theta_i, \phi_i). \quad \text{(A26)}$$

In particular, the restrictions of $\psi^{\epsilon_j}_{mn}(qr_j, \theta_j, \phi_j)$ and of its normal derivative onto $\partial\Omega_i$ involve the matrices $\tilde{\mathbf{p}}, \tilde{\mathbf{q}}$ and $\tilde{\mathbf{p}}', \tilde{\mathbf{q}}'$, respectively, see Eqs. (A24).

As the vectors $\boldsymbol{L}_{ij}$ and $\boldsymbol{L}_{ji}$ have opposite directions, one has

$$\psi^{\pm}_{mn}(qL_{ij}, \Theta_{ij}, \Phi_{ij}) = (-1)^n \psi^{\pm}_{mn}(qL_{ji}, \Theta_{ji}, \Phi_{ji}). \quad \text{(A27)}$$

Using the symmetry properties of Clebsch-Gordan coefficients (see Ref.[93], Section 27.9), one can show that the matrix $\mathbf{U}$ is Hermitian: $\mathbf{U}^\dagger = \mathbf{U}^*$. As a consequence, one has

$$\mathbf{W}^{\dagger,*} = \mathbf{q} + \mathbf{p}\mathbf{U}. \quad \text{(A28)}$$

3. Matrix elements F^i_{mn} for the Green function

In order to compute the matrix elements F^i_{mn} needed for the evaluation of the Green function, we use the following expansion of the fundamental solution (derived from Ref.[92]):

$$G_{\mathrm{f}}(\boldsymbol{x}, \boldsymbol{y}; q) = \begin{cases} q \displaystyle\sum_{n=0}^{\infty} \sum_{m=-n}^{n} (-1)^m \psi^+_{(-m)n}(qr_0, \theta_0, \phi_0)\, \psi^-_{mn}(qr, \theta, \phi) & (r_0 < r), \\ q \displaystyle\sum_{n=0}^{\infty} \sum_{m=-n}^{n} (-1)^m \psi^-_{mn}(qr_0, \theta_0, \phi_0)\, \psi^+_{(-m)n}(qr, \theta, \phi) & (r_0 > r), \end{cases} \quad \text{(A29)}$$

where (r,θ,ϕ) and (r_0,θ_0,ϕ_0) are respectively the spherical coordinates of $\boldsymbol{x}$ and $\boldsymbol{y}$ with respect to the origin. Since the fundamental solution is translationally invariant, i.e., $G_{\rm f}(\boldsymbol{x},\boldsymbol{y};q)=G_{\rm f}(\boldsymbol{x}-\boldsymbol{x}_i,\boldsymbol{y}-\boldsymbol{x}_i;q)$ for any vector $\boldsymbol{x}_i$, one can apply Eqs. (A29) to represent $G_{\rm f}(\boldsymbol{x},\boldsymbol{y};q)$ in the local spherical coordinates of the ball Ω_i (with $i=1,2,\ldots,N$):

$$G_{\rm f}(\boldsymbol{x},\boldsymbol{y};q)=q\sum_{m,n}\boldsymbol{\Psi}^{i,*}_{mn}(\boldsymbol{y})\,\psi^{+}_{mn}(qr_i,\theta_i,\phi_i)\quad(r_i<L_i),\tag{A30}$$

in which we introduced the (row) vector $\boldsymbol{\Psi}(\boldsymbol{y})$ with the components

$$\boldsymbol{\Psi}^{i}_{mn}(\boldsymbol{y})=\psi^{\epsilon_i}_{mn}(qL_i,\Theta_i,\Phi_i),\tag{A31}$$

where (L_i,Θ_i,Φ_i) are the local spherical coordinates of $\boldsymbol{y}$ with respect to the ball Ω_i for $i=0,1,\ldots,N$ (i.e., the spherical coordinates of the vector $\boldsymbol{y}-\boldsymbol{x}_i$). In addition, to replace $(-1)^m\psi_{(-m)n}$ by ψ^*_{mn}, we used the following identity for the normalized spherical harmonics:

$$Y_{(-m)n}(\theta,\phi)=(-1)^m\,Y^*_{mn}(\theta,\phi),\tag{A32}$$

which follows from the identity for associated Legendre polynomials:

$$P_n^{-m}(x)=(-1)^m\frac{(n-m)!}{(n+m)!}\,P_n^m(x).\tag{A33}$$

From Eq. (A30), we determine f_i according to Eq. (9):

$$f_i=q\sum_{m,n}\boldsymbol{\Psi}^{i,*}_{mn}(\boldsymbol{y})\big(a_i i_n(qR_i)-b_iR_i\,q\,i_n'(qR_i)\big)Y_{mn}(\theta_i,\phi_i)\tag{A34}$$

and thus

$$F^i_{mn}=q\boldsymbol{\Psi}^{i,*}_{mn}(\boldsymbol{y})\big(a_i i_n(qR_i)-b_iR_i\,q\,i_n'(qR_i)\big).\tag{A35}$$

Similarly, the representation of $G_{\rm f}(\boldsymbol{x},\boldsymbol{y};q)$ in the local spherical coordinates of the ball Ω_0 reads

$$G_{\rm f}(\boldsymbol{x},\boldsymbol{y};q)=q\sum_{m,n}\boldsymbol{\Psi}^{0,*}_{mn}(\boldsymbol{y})\psi^{-}_{mn}(qr_0,\theta_0,\phi_0)\quad(r_0>L_0),\tag{A36}$$

from which we get

$$f_0=q\sum_{m,n}\boldsymbol{\Psi}^{0,*}_{mn}(\boldsymbol{y})\big(a_0k_n(qR_0)+b_0R_0\,q\,k_n'(qR_0)\big)\times Y_{mn}(\theta_0,\phi_0),\tag{A37}$$

and thus

$$F^0_{mn}=q\boldsymbol{\Psi}^{0,*}_{mn}(\boldsymbol{y})\big(a_0k_n(qR_0)+b_0R_0\,q\,k_n'(qR_0)\big).\tag{A38}$$

Using the matrix $\mathbf{p}$ from Eq. (A24a), one can represent the vector $\mathbf{F}$ as

$$\mathbf{F}=q\boldsymbol{\Psi}^*(\boldsymbol{y})\mathbf{p}.\tag{A39}$$

4. Normal derivative of the solution

Once the coefficients A^i_{mn} are found, one can easily evaluate the solution $w(\boldsymbol{x};q)$ and its derivatives in any point $\boldsymbol{x}$. For many applications, one needs to compute the restriction of the solution and the flux onto the boundary $\partial\Omega$ which requires finding the normal derivative of $w(\boldsymbol{x};q)$.

Using Eq. (A26) with $a_i=1$ and $b_iR_i=0$, one gets immediately

$$w|_{\partial\Omega_i}=\sum_{m,n}\big(\mathbf{A}\tilde{\mathbf{W}}\big)^i_{mn}\,Y_{mn}(\theta_i,\phi_i),\tag{A40}$$

where

$$\tilde{\mathbf{W}}=\tilde{\mathbf{q}}+\mathbf{U}\tilde{\mathbf{p}},\tag{A41}$$

with matrices $\tilde{\mathbf{p}}$ and $\tilde{\mathbf{q}}$ given by Eqs. (A25). In turn, setting $a_i=0$ and $b_iR_i=1$ in Eq. (A26), one has

$$\left(\frac{\partial w}{\partial\boldsymbol{n}}\right)\Big|_{\partial\Omega_i}=\sum_{m,n}\big(\mathbf{A}\tilde{\mathbf{W}}'\big)^i_{mn}\,Y_{mn}(\theta_i,\phi_i),\tag{A42}$$

where

$$\tilde{\mathbf{W}}'=\tilde{\mathbf{q}}'+\mathbf{U}\tilde{\mathbf{p}}'.\tag{A43}$$

As a particular application, we evaluate the normal derivative of the Green function $G(\boldsymbol{x},\boldsymbol{y};q)$. Using the expansions (5, A30), we get for $i>0$:

$$\frac{\partial G(\boldsymbol{x},\boldsymbol{y};q)}{\partial\boldsymbol{n}}\Big|_{\partial\Omega_i}=-\sum_{m,n}\Big\{\big(q\boldsymbol{\Psi}^{i,*}_{mn}(\boldsymbol{y})-(\mathbf{AU})^i_{mn}\big)qi_n'(qR_i)-A^i_{mn}qk_n'(qR_i)\Big\}Y_{mn}(\theta_i,\phi_i),\tag{A44}$$

where $\boldsymbol{\Psi}^i_{mn}(\boldsymbol{y})$ are given explicitly by Eq. (A31), and

$$\frac{\partial G(\boldsymbol{x},\boldsymbol{y};q)}{\partial\boldsymbol{n}}\Big|_{\partial\Omega_0}=\sum_{m,n}\Big\{\big(q\boldsymbol{\Psi}^{0,*}_{mn}(\boldsymbol{y})-(\mathbf{AU})^0_{mn}\big)qk_n'(qR_0)-A^0_{mn}qi_n'(qR_0)\Big\}Y_{mn}(\theta_0,\phi_0).\tag{A45}$$

Using the matrices $\tilde{\mathbf{p}}'$ and $\tilde{\mathbf{q}}'$ from Eqs. (A25) and the expressions (13, A39), the above relations can be written together (for any $i=0,1,\ldots,N$) as

$$\frac{\partial G(\boldsymbol{x},\boldsymbol{y};q)}{\partial\boldsymbol{n}}\Big|_{\partial\Omega_i}=-\sum_{m,n}\mathbf{J}^i_{mn}(\boldsymbol{y})\,Y_{mn}(\theta_i,\phi_i),\tag{A46}$$

where

$$\mathbf{J}(\boldsymbol{y})=q\boldsymbol{\Psi}^*(\boldsymbol{y})\Big(\mathbf{p}(\mathbf{q}+\mathbf{Up})^{-1}(\tilde{\mathbf{q}}'+\mathbf{U}\tilde{\mathbf{p}}')-\tilde{\mathbf{p}}'\Big).\tag{A47}$$

It is also convenient to represent the matrix in the large parentheses as

$$\mathbf{p}(\mathbf{q}+\mathbf{Up})^{-1}(\tilde{\mathbf{q}}'+\mathbf{U}\tilde{\mathbf{p}}')-\tilde{\mathbf{p}}'=(\mathbf{q}+\mathbf{pU})^{-1}(\mathbf{p}\tilde{\mathbf{q}}'-\mathbf{q}\tilde{\mathbf{p}}').\tag{A48}$$

To proof this identity, both sides can be multiplied by $(\mathbf{q}+\mathbf{pU})$ on the left to get

$$(\mathbf{q}+\mathbf{pU})\mathbf{p}(\mathbf{q}+\mathbf{Up})^{-1}(\tilde{\mathbf{q}}'+\mathbf{U}\tilde{\mathbf{p}}')-(\mathbf{q}+\mathbf{pU})\tilde{\mathbf{p}}' = \mathbf{p}\tilde{\mathbf{q}}'-\mathbf{q}\tilde{\mathbf{p}}'.$$

As the matrices $\mathbf{p}$ and $\mathbf{q}$ are diagonal, they commute, and one has

$$(\mathbf{q}+\mathbf{pU})\mathbf{p}(\mathbf{q}+\mathbf{Up})^{-1} = \mathbf{p}(\mathbf{p}^{-1}\mathbf{q}+\mathbf{U})(\mathbf{q}\mathbf{p}^{-1}+\mathbf{U})^{-1} = \mathbf{p},$$

from which the identity (A48) follows. Moreover, the last matrix in Eq. (A48) has a particularly simple form:

$$\left(\mathbf{p}\tilde{\mathbf{q}}' - \mathbf{q}\tilde{\mathbf{p}}'\right)^{ij}_{mn,kl} = \delta_{ij}\delta_{nl}\delta_{mk}\frac{a_j}{qR_j^2}\,, \tag{A49}$$

which is easily obtained by using the Wronskian (36). We conclude that

$$\mathbf{J}^i_{mn}(\boldsymbol{y}) = \frac{a_i}{R_i^2}\left(\mathbf{\Psi}^*(\boldsymbol{y})(\mathbf{q}+\mathbf{pU})^{-1}\right)^i_{mn}. \tag{A50}$$

5. Integration of the solution

The re-expansion theorems allow one to easily integrate the solution $w(\boldsymbol{x};q)$ of the modified Helmholtz equation over balls or spheres. In fact, one can re-expand basis functions $\psi^{\pm}_{mn}$ in Eq. (5) on the appropriate basis functions in the local spherical coordinate of a ball or a sphere, over which the integral needs to be evaluated. After that, the integral can be evaluated explicitly. To illustrate this computation, we find the integral of the solution $w(\boldsymbol{x};q)$ over the whole domain Ω, which is a more complicated setting. For this purpose, one needs to compute the integrals:

$$\overline{\psi}^j_{mn} = \int_\Omega d\boldsymbol{x}\,\psi^{\epsilon_j}_{mn}(qr_j,\theta_j,\phi_j) \tag{A51}$$

for $j = 0,1,2,\ldots,N$ (we recall that $\epsilon_j = -$ for $j>0$ and $\epsilon_0 = +$). The following computation relies on the additivity of the integral over $\Omega = \Omega_0\backslash\cup_{i=1}^N\overline{\Omega}_i$, with non-overlapping balls. For $j>0$, one can split the integral over Ω into three parts:

$$\begin{aligned}\overline{\psi}^j_{mn} = &\int_{\mathbb{R}^3\backslash\Omega_j} d\boldsymbol{x}\,\psi^-_{mn}(qr_j,\theta_j,\phi_j) - \int_{\mathbb{R}^3\backslash\Omega_0} d\boldsymbol{x}\,\psi^-_{mn}(qr_j,\theta_j,\phi_j)\\ &- \sum_{i=1,i\neq j}^N \int_{\Omega_i} d\boldsymbol{x}\,\psi^-_{mn}(qr_j,\theta_j,\phi_j)\end{aligned}$$

(for the exterior problem, $\Omega_0 = \mathbb{R}^3$, and there is no second term). The first term can be easily computed due to orthogonality of spherical harmonics. In turn, one uses the II and IR re-expansion theorems (A13, A15) for the second and the third terms, respectively, in order to switch to the local spherical coordinates of the integration domain. After that, the corresponding basis functions can be easily integrated. We get

$$\begin{aligned}\overline{\psi}^j_{mn} = \frac{\sqrt{4\pi}}{q}\Big(&\delta_{n0}\delta_{m0}R_j^2 k_1(qR_j) - U^{(-j,-0)}_{mn,00}R_0^2 k_1(qR_0)\\ &- \sum_{i=1,i\neq j}^N U^{(-j,+i)}_{mn,00}R_i^2 i_1(qR_i)\Big),\end{aligned} \tag{A52}$$

where $i_1(z)$ and $k_1(z)$ came from the integrals of $r^2 i_0(qr)$ and $r^2 k_0(qr)$, respectively. Similarly, we use the RR re-expansion theorem (A11) to get

$$\overline{\psi}^0_{mn} = \frac{\sqrt{4\pi}}{q}\left(\delta_{n0}\delta_{m0}R_0^2 i_1(qR_0) - \sum_{i=1}^N U^{(+0,+i)}_{mn,00}R_i^2 i_1(qR_i)\right). \tag{A53}$$

For instance, these expressions help to find the components of the vector $\overline{\mathbf{J}}$ used in Eq. (43):

$$\begin{aligned}\overline{\mathbf{J}}^i_{mn} &= \int_\Omega d\boldsymbol{y}\,\mathbf{J}^i_{mn}\\ &= \frac{a_i}{R_i^2}\int_\Omega d\boldsymbol{y}\sum_{j=0}^N\sum_{k,l}\mathbf{\Psi}^{j,*}_{kl}(\boldsymbol{y})\left((\mathbf{q}+\mathbf{pU})^{-1}\right)^{ji}_{kl,mn}\\ &= \frac{a_i}{R_i^2}\left(\overline{\mathbf{\Psi}}^*(\mathbf{q}+\mathbf{pU})^{-1}\right)^i_{mn},\end{aligned} \tag{A54}$$

where the vector $\overline{\mathbf{\Psi}}$ is formed by $\overline{\psi}^j_{mn}$.

Appendix B: Practical implementation

A practical implementation of the GMSV requires a truncation of all involved matrices. If $n_{\max}$ denotes the truncation order for expansions over spherical harmonics (i.e., one keeps the terms with $n = 0,1,2\ldots,n_{\max}$), then the number of unknown coefficients A^i_{mn} for each i is $(n_{\max}+1)^2$ that accounts for the second index m running from $-n$ to n. In total, there are $(N+1)(n_{\max}+1)^2$ unknown coefficients A^i_{mn}, with $i = 0,1,\ldots N$. As discussed in detail in Ref.[31], the coefficients A^i_{mn} can be re-ordered to form a (row) vector as

$$\begin{aligned}\mathbf{A} = \{&\overbrace{A^0_{0,0}}^{1},\ \overbrace{A^0_{-1,0},A^0_{0,0},A^0_{1,0}}^{3},\ldots,\overbrace{A^0_{-n,n},\ldots,A^0_{n,n}}^{2n+1},\ldots,\\ &A^1_{0,0},\ A^1_{-1,0},A^1_{0,0},A^1_{1,0},\ldots,A^1_{-n,n},\ldots,A^1_{n,n},\ldots,\\ &\ldots\qquad\ldots\qquad\ldots\\ &A^N_{0,0},\ A^N_{-1,0},A^N_{0,0},A^N_{1,0},\ldots,A^N_{-n,n},\ldots,A^N_{n,n},\ldots\}\end{aligned}$$

Using the same re-ordering scheme, one can build the matrix $\mathbf{W}$ of size $(N+1)(n_{\max}+1)^2\times(N+1)(n_{\max}+1)^2$. For the exterior problem, there is no outer boundary $\partial\Omega_0$, all $A^0_{mn}\equiv 0$, and the size of the matrix is reduced to $N(n_{\max}+1)^2\times N(n_{\max}+1)^2$. While larger truncation order $n_{\max}$ yields more accurate results, the computational time grows very rapidly with $n_{\max}$, particularly

due to the matrix inversion. When both N and $n_{\max}$ need to be large, the basic implementation of the GMSV is prohibitly time-consuming, and one needs to rely on advanced implementations (see the related discussion in Ref.[31]), e.g., the matrix inversion should be implemented by iterative methods, while fast multipole methods can be employed[39,40,50,77–81]. At the same time, quite accurate results can often be achieved with small $n_{\max}$ (see, e.g., Fig. 4).

1. Limits $q \to 0$ and $q \to \infty$

In the limit $q \to 0$, the modified Helmholtz equation is reduced to the Laplace equation, whereas the presented method becomes identical with that from Ref.[31]. In particular, the basis functions $\psi^{\pm}_{mn}$ are reduced to the basis functions satisfying the Laplace equation:

$$q^{-n}\psi^{+}_{mn}(qr_i,\theta_i,\phi_i) \to \frac{\sqrt{\pi}}{2^{n+1}\Gamma(n+3/2)}\, r_i^n Y_{mn}(\theta_i,\phi_i),$$
$$q^{n+1}\psi^{-}_{mn}(qr_i,\theta_i,\phi_i) \to \frac{2^n\Gamma(n+1/2)}{\sqrt{\pi}}\, r_i^{-n-1} Y_{mn}(\theta_i,\phi_i),$$

where we used the asymptotic behavior of the modified spherical Bessel functions. The re-expansion theorems and the elements of all the matrices can thus be recalculated (see[31] for details[†]). However, it should be noted that the singular behavior of the basis functions $\psi^{-}_{mn}(qr_i,\theta_i,\phi_i)$ as $q \to 0$ may cause numerical errors and instabilities for small q, in particular, in the matrix inversion. This issue should be carefully addressed upon the implementation.

In the opposite limit of large q, the regular basis functions $\psi^{+}_{mn}(qr_i,\theta_i,\phi_i)$ grow as $\exp(qr_i)$, whereas $\psi^{-}_{mn}(qr_i,\theta_i,\phi_i)$ decays as $\exp(-qr_i)$. This exponential behavior may also cause numerical instabilities that can be amended by rescaling modified spherical Bessel function by appropriate exponential factors that can be treated explicitly. When the balls are well separated from each other, their diffusion interaction is dramatically reduced in this limit, and the solution can become much simpler. These simplifications can be helpful for investigating the asymptotic behavior as $q \to \infty$.

2. Recurrence relations

The direct computation of the translation matrix $\mathbf{U}$ via explicit Eqs. (A11, A13, A15) is time-consuming because these formulas require numerous evaluations of modified spherical Bessel functions, spherical harmonics, and Clebsch-Gordan coefficients. The computational time can be considerably reduced by adapting the recurrence relations that were originally derived by Chew[76] for the elements $\tilde{U}^{(+j,+i)}_{mn,kl}$ of the translation operator for regular basis functions $\tilde{\psi}^{+}_{mn}$ of the ordinary Helmholtz equation (see Eq. (A3)):

$$a^{+}_{mn}\beta_{kl,m(n+1)} = -a^{-}_{mn}\beta_{kl,m(n-1)} + a^{+}_{k(l-1)}\beta_{k(l-1),mn} + a^{-}_{k(l+1)}\beta_{k(l+1),mn}, \tag{B1}$$

$$b^{+}_{mn}\beta_{kl,(m+1)(n+1)} = -b^{-}_{mn}\beta_{kl,(m+1)(n-1)} + b^{+}_{(k-1)(l-1)}\beta_{(k-1)(l-1),mn} + b^{-}_{(k-1)(l+1)}\beta_{(k-1)(l+1),mn}, \tag{B2}$$

where

$$a^{+}_{mn} = -\left(\frac{(n+1+m)(n+1-m)}{(2n+1)(2n+3)}\right)^{1/2},$$
$$a^{-}_{mn} = \left(\frac{(n+m)(n-m)}{(2n+1)(2n-1)}\right)^{1/2},$$
$$b^{+}_{mn} = \left(\frac{(n+m+2)(n+m+1)}{(2n+1)(2n+3)}\right)^{1/2},$$
$$b^{-}_{mn} = \left(\frac{(n-m)(n-m-1)}{(2n+1)(2n-1)}\right)^{1/2}$$

for $|m| \le n$, and 0 otherwise[76] (here, $\beta_{kl,mn}$ is a shortcut notation for $\tilde{U}^{(+j,+i)}_{mn,kl}$, see below). Later, Gumerov and Duraiswami re-derived these relations and also applied them to two other (IR and RR) re-expansion theorems[39,94].

As these recurrence relations result from the recurrence relations for spherical Bessel functions and spherical harmonics, they are also valid for the basis functions $\psi^{\pm}_{mn}$ of the modified Helmholtz equations. However, we could not find earlier derivations of such recurrence relations in this setting. Skipping tedious mathematical details (which are similar to that presented in[76,94]), we briefly

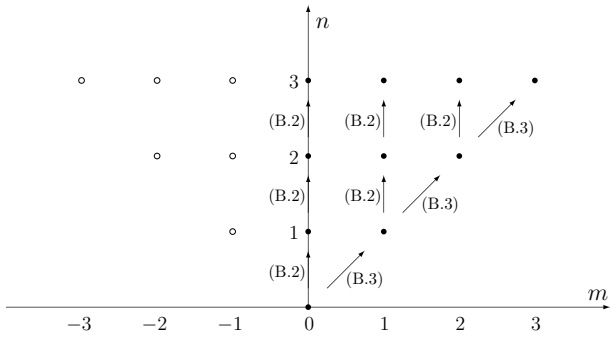

FIG. 6: Schematic order of the recurrence computation of $\beta_{kl,mn}$. From the initialized values of $\beta_{kl,00}$ at $m = n = 0$, one first computes the sectorial elements $\beta_{kl,nn}$ with $n = 1, 2, \ldots, n_{\max}$ by using Eq. (B2). Then, for each $m = 1, 2, \ldots, n_{\max}$, one moves along the m-th vertical line, from $n = m$ to $n = n_{\max}$, using Eq. (B1). In parallel, the values for negative m are computed via Eq. (B4).

[†] Since non-normalized spherical harmonics were used in Ref.[31], its formulas have to be renormalized via the normalization factor in Eq. (8) to coincide with formulas presented here.

explain the use of these relations for computing the elements of the translation matrices $U^{(\pm j,\pm i)}_{mn,kl}$.

Let us start from the RR re-expansion theorem. For given indices (k,l), we aim at computing recursively the elements $\beta_{kl,mn}$ for all $0\le n\le n_{\max}$ and $|m|\le n$, where $n_{\max}$ is the truncation order. The starting point is the identity

$$\beta_{kl,00}=\sqrt{4\pi}\,(-1)^k\,i^l\,\underbrace{i_l(qL_{ij})\,Y_{(-k)l}(\Theta_{ij},\Phi_{ij})}_{\psi^+_{(-k)l}(qL_{ij},\Theta_{ij},\Phi_{ij})},\qquad \text{(B3)}$$

which follows from Eq. (A12) (here we keep using the shorter notation $\beta_{kl,mn}$ instead of $U^{(+j,+i)}_{mn,kl}$; they slightly differ and will be related by Eq. (B5)). First, one evaluates the "sectorial" elements $\beta_{kl,nn}$ via the relation (B2). Since $b^-_{nn}=0$, the first term on the right-hand side is canceled, and this relation expresses $\beta_{kl,(n+1)(n+1)}$ in terms of $\beta_{k'l',nn}$ with different indices (k',l'). As a consequence, each step of the recursive computation should be performed for the whole set of indices (k',l'). Once the sectorial elements are found, one can use the relation (B1) to express $\beta_{kl,m(n+1)}$ in terms of already known $\beta_{k'l',mn}$ and $\beta_{k'l',m(n-1)}$ (see Fig. 6). In this way, one can compute all the elements up to the truncation order $n_{\max}$. Note that the elements for negative m can be found from

$$\beta_{kl,(-m)n}=(-1)^{k+l+m+n}\beta^*_{(-k)l,mn}.\qquad \text{(B4)}$$

We also stress that the computation of the element $\beta_{kl,n_{\max}n_{\max}}$ via $n_{\max}$ repeated applications of Eq. (B2) involves the element $\beta_{(k-n_{\max})(l+n_{\max}),00}$, so that for $l=n_{\max}$, one needs to know $\beta_{(k-n_{\max})(2n_{\max}),00}$. As a consequence, even if the truncation order is $n_{\max}$ and the translation matrix β has to be of the size $(n_{\max}+1)^2\times(n_{\max}+1)^2$, intermediate computations involve the elements of the order up to $2n_{\max}$.

Once the matrix elements $\beta_{kl,mn}$ are computed, one gets

$$U^{(+j,+i)}_{mn,kl}=(-i)^{l-n}\beta_{kl,mn}.\qquad \text{(B5)}$$

Similarly, one obtains the matrix elements for the II re-expansion theorem:

$$U^{(-j,-i)}_{mn,kl}=i^{l-n}\beta_{kl,mn},\qquad \text{(B6)}$$

which differ only by the sign factor.

Finally, in the case of the IR re-expansion theorem, the recurrence relations are the same but they have to be initialized by using the irregular basis function:

$$\tilde\beta_{kl,00}=\sqrt{4\pi}\,(-1)^{k+l}i^l\,\underbrace{k_l(qL_{ij})\,Y_{(-k)l}(\Theta_{ij},\Phi_{ij})}_{\psi^-_{(-k)l}(qL_{ij},\Theta_{ij},\Phi_{ij})}\qquad \text{(B7)}$$

(the tilde distinguishes the matrix elements with this initialization from the former ones). Once such $\tilde\beta_{kl,mn}$ are found using the above relations, one gets

$$U^{(-j,+i)}_{mn,kl}=i^{l-n}(-1)^l\tilde\beta_{kl,mn}.\qquad \text{(B8)}$$

Note that modified spherical Bessel functions, their derivatives, and spherical harmonics can also be found via standard recurrence relations.

3. Numerical inversion of the Laplace transform

Throughout this paper, we focused on solving the modified Helmholtz equation and thus getting solutions of time-dependent diffusion problems in the Laplace domain. For instance, Sec. III provides semi-analytical representations for Laplace-transformed probability flux density $\tilde j(\boldsymbol{s},p|\boldsymbol{y})$, first-passage time density $\tilde H(p|\boldsymbol{y})$ and reaction rate $\tilde J(p)$. Even so these quantities present their own interest, the natural next step consists in inverting the Laplace transform to get back to time domain. For this purpose, one needs to compute the Bromwich integral over a contour in the complex plane, either numerically, or via the residue theorem. In both cases, one has to evaluate the quantity of interest (e.g., $\tilde J(p)$) at $p\in\mathbb{C}$, which requires extending the presented GMSV to $q\in\mathbb{C}$, i.e., beyond the declared assumption of nonnegative q, see Sec. II A. In particular, some formulas have to be adapted to be valid for $q\in\mathbb{C}$. Without pretending for generality and rigor, we briefly discuss several lines of such extension.

Basically, one needs to check the validity of relations with complex conjugation. For instance, in Eq. (A30), we wrote $\boldsymbol{\Psi}^{i,*}_{mn}$ instead of $(-1)^m\boldsymbol{\Psi}^i_{(-m)n}$ which stood in Eq. (A29). This identification came from Eq. (A32) for spherical harmonics and is valid for a real q, but fails for a complex q. In other words, in all relations containing $\boldsymbol{\Psi}^*$, one has to replace $\boldsymbol{\Psi}^{i,*}_{mn}$ by $(-1)^m\boldsymbol{\Psi}^i_{(-m)n}$ to make it valid for a complex q (the same for $\overline{\boldsymbol{\Psi}}^*$). Similarly, we employed Eq. (B4), which is valid for a real q but fails for a complex q. For evaluating $\beta_{kl,(-m)n}$ with a complex q, one can still rely on Eq. (B1) with negative m. In turn, the evaluation of the sectorial element $\beta_{kl,-(n+1)(n+1)}$ can be performed by replacing Eq. (B2) by

$$\begin{aligned}b^+_{mn}\beta_{kl,(-m-1)(n+1)}=&-b^-_{mn}\beta_{kl,(-m-1)(n-1)}\\&+b^+_{(-k-1)(l-1)}\beta_{(k+1)(l-1),(-m)n}\\&+b^-_{(-k-1)(l+1)}\beta_{(k+1)(l+1),(-m)n}.\end{aligned}\qquad \text{(B9)}$$

This modification allows one to evaluate the matrix elements of the translation operators for complex q and thus to apply numerical algorithms for inverting the Laplace transform.

Appendix C: Two concentric spheres

In this Appendix, we illustrate the use of the GMSV for a domain between two concentric spheres of radii $R_1<R_0$, for which the inversion of the matrix $\mathbf{W}$ can

be performed explicitly. In this domain, one has

$$\mathbf{U}^{(+0,+1)}_{mn,kl} = \delta_{ln}\delta_{mk}\, b^0_{nmnm}/\sqrt{4\pi},$$
$$\mathbf{U}^{(-1,-0)}_{mn,kl} = \delta_{ln}\delta_{mk}\, b^n_{nm00}/\sqrt{4\pi},$$

because $L_{12}=0$ and we used $i_\nu(0)=\delta_{0\nu}$. Since $b^0_{nmnm} = b^n_{nm00} = \sqrt{4\pi}$, one finds $\mathbf{U}^{(+0,+1)} = \mathbf{U}^{(-1,-0)} = \mathbf{I}$ and thus

$$(\mathbf{q}+\mathbf{U}\mathbf{p})^{ij}_{mn,kl} = \delta_{ln}\delta_{mk} v^{ij}_n, \tag{C1}$$

with

$$v^{00}_n = a_0 i_n(qR_0) + b_0 R_0\, q\, i'_n(qR_0), \tag{C2a}$$
$$v^{01}_n = a_1 i_n(qR_1) - b_1 R_1\, q\, i'_n(qR_1), \tag{C2b}$$
$$v^{10}_n = a_0 k_n(qR_0) + b_0 R_0\, q\, k'_n(qR_0), \tag{C2c}$$
$$v^{11}_n = a_1 k_n(qR_1) - b_1 R_1\, q\, k'_n(qR_1). \tag{C2d}$$

Inverting the block diagonal matrix, we find

$$\left(\mathbf{W}^{-1}\right)^{ij}_{klmn} = \delta_{ln}\delta_{mk}\, w^{ij}_n, \tag{C3}$$

with

$$w^{00}_n = v^{11}_n/w_n, \qquad w^{01}_n = -v^{01}_n/w_n,$$
$$w^{10}_n = -v^{10}_n/w_n, \qquad w^{11}_n = v^{00}_n/w_n,$$

where

$$w_n = v^{00}_n v^{11}_n - v^{01}_n v^{10}_n. \tag{C4}$$

1. Green function

If one aims at computing the Green function $G(\boldsymbol{x},\boldsymbol{y};q)$, one also finds

$$F^0_{mn} = q\, i_n(qL_0)\, Y^*_{mn}(\Theta_0,\Phi_0)\, v^{10}_n, \tag{C5a}$$
$$F^1_{mn} = q\, k_n(qL_0)\, Y^*_{mn}(\Theta_0,\Phi_0)\, v^{01}_n, \tag{C5b}$$

where (L_0,Θ_0,Φ_0) are the spherical coordinates of $\boldsymbol{y}$ (we recall that both spheres are centered at the origin). As a consequence, one gets the coefficients:

$$A^0_{mn} = q\, Y^*_{mn}(\Theta_0,\Phi_0) \times \left(\frac{v^{10}_n v^{11}_n}{w_n} i_n(qL_0) - \frac{v^{10}_n v^{01}_n}{w_n} k_n(qL_0)\right), \tag{C6a}$$

$$A^1_{mn} = q\, Y^*_{mn}(\Theta_0,\Phi_0) \times \left(-\frac{v^{01}_n v^{10}_n}{w_n} i_n(qL_0) + \frac{v^{00}_n v^{01}_n}{w_n} k_n(qL_0)\right). \tag{C6b}$$

Substituting these coefficients into Eq. (5), we get the Green function from Eqs. (4, 15):

$$G(\boldsymbol{x},\boldsymbol{y};q) = G_{\rm f}(\boldsymbol{x},\boldsymbol{y};q) - \frac{q}{4\pi}\sum_{n=0}^{\infty}(2n+1)P_n\left(\frac{(\boldsymbol{x}\cdot\boldsymbol{y})}{|\boldsymbol{x}|\,|\boldsymbol{y}|}\right) \times \left\{\left(\frac{v^{10}_n v^{11}_n}{w_n} i_n(q|\boldsymbol{y}|) - \frac{v^{10}_n v^{01}_n}{w_n} k_n(q|\boldsymbol{y}|)\right) i_n(q|\boldsymbol{x}|) - \left(\frac{v^{01}_n v^{10}_n}{w_n} i_n(q|\boldsymbol{y}|) - \frac{v^{00}_n v^{01}_n}{w_n} k_n(q|\boldsymbol{y}|)\right) k_n(q|\boldsymbol{x}|)\right\}, \tag{C7}$$

where $P_n(z)$ are Legendre polynomials, and we used the addition theorem for spherical harmonics to perform the sum over m:

$$\sum_{m=-n}^{n} Y_{mn}(\theta,\phi)Y^*_{mn}(\Theta_0,\Phi_0) = \frac{2n+1}{4\pi}P_n\left(\frac{(\boldsymbol{x}\cdot\boldsymbol{y})}{|\boldsymbol{x}|\,|\boldsymbol{y}|}\right). \tag{C8}$$

This general expression is reduced to two limiting cases:

(i) an interior problem inside a sphere of radius R_0 corresponds to the limit $R_1\to 0$, in which $v^{01}_n\to 0$ while $v^{11}_n\to\infty$ so that

$$G(\boldsymbol{x},\boldsymbol{y};q) = G_{\rm f}(\boldsymbol{x},\boldsymbol{y};q) - \frac{q}{4\pi}\sum_{n=0}^{\infty}(2n+1)P_n\left(\frac{(\boldsymbol{x}\cdot\boldsymbol{y})}{|\boldsymbol{x}|\,|\boldsymbol{y}|}\right) \times \frac{a_0 k_n(qR_0) + b_0 R_0 q k'_n(qR_0)}{a_0 i_n(qR_0) + b_0 R_0 q i'_n(qR_0)}\, i_n(q|\boldsymbol{x}|)\, i_n(q|\boldsymbol{y}|); \tag{C9}$$

(ii) an exterior problem outside one sphere of radius R_1 corresponds to the limit $R_0\to\infty$, in which $v^{10}_n\to 0$ while $v^{00}_n\to\infty$ so that

$$G(\boldsymbol{x},\boldsymbol{y};q) = G_{\rm f}(\boldsymbol{x},\boldsymbol{y};q) - \frac{q}{4\pi}\sum_{n=0}^{\infty}(2n+1)P_n\left(\frac{(\boldsymbol{x}\cdot\boldsymbol{y})}{|\boldsymbol{x}|\,|\boldsymbol{y}|}\right) \times \frac{a_1 i_n(qR_1) - b_1 R_1 q i'_n(qR_1)}{a_1 k_n(qR_1) - b_1 R_1 q k'_n(qR_1)}\, k_n(q|\boldsymbol{x}|)\, k_n(q|\boldsymbol{y}|). \tag{C10}$$

Note that the distribution of the reaction time for two concentric spheres was studied in Ref.[95].

2. Dirichlet-to-Neumann operator

Using the above explicit relations, we also compute the matrix $\mathbf{M}$ determining the spectrum of the Dirichlet-to-Neumann operator:

$$(\mathbf{M})_{mn,kl} = \delta_{nl}\delta_{mk}\frac{q}{w_n}\times \begin{pmatrix} v^{11}_n i'_n(qR_0) - v^{01}_n k'_n(qR_0) & -v^{11}_n i'_n(qR_1) + v^{01}_n k'_n(qR_1) \\ -v^{10}_n i'_n(qR_0) + v^{00}_n k'_n(qR_0) & v^{10}_n i'_n(qR_1) - v^{00}_n k'_n(qR_1) \end{pmatrix}. \tag{C11}$$

Let us first consider the case when only the inner sphere is reactive whereas the outer sphere is reflecting. Substituting $a_0=0$, $a_1=1$, $b_0=1$, $b_1=0$ into Eqs. (C2), we get

$$(\mathbf{M})_{mn,kl} = \delta_{nl}\delta_{mk} \times \begin{pmatrix} 1/R_0 & -1/(qR_1)^2/R_0 \\ 0 & q\frac{k'_n(qR_0)i'_n(qR_1) - i'_n(qR_0)k'_n(qR_1)}{k_n(qR_1)i'_n(qR_0) - i_n(qR_1)k'_n(qR_0)} \end{pmatrix}. \tag{C12}$$

The diagonal structure of this matrix allows one to easily determine its eigenvalues:

$$\mu^{(p)}_n = q\frac{k'_n(qR_0)i'_n(qR_1) - i'_n(qR_0)k'_n(qR_1)}{k_n(qR_1)i'_n(qR_0) - i_n(qR_1)k'_n(qR_0)}, \tag{C13}$$

where $q = \sqrt{p/D}$. Note that this matrix also has infinitely many spurious eigenvalues $1/R_0$, which come from the redundant form of the matrix $\mathbf{M}$ in this setting with Neumann condition. Similarly, one can treat the case when only the outer sphere is reactive.

When both spheres are reactive, one substitutes $a_0 = a_1 = 1$ and $b_0 = b_1 = 0$ into Eqs. (C2) to get

$$(\mathbf{M})_{mn,kl} = \frac{\delta_{nl}\delta_{mk}\, q}{i_n(qR_0)k_n(qR_1) - i_n(qR_1)k_n(qR_0)} \times \begin{pmatrix} k_n(qR_1)i'_n(qR_0) - i_n(qR_1)k'_n(qR_0) & -1/(qR_1)^2 \\ -1/(qR_0)^2 & k_n(qR_0)i'_n(qR_1) - i_n(qR_0)k'_n(qR_1) \end{pmatrix}. \tag{C14}$$

The eigenvalues are obtained by diagonalizing separately each 2×2 block of this matrix and can be expressed as solutions of the associated quadratic equation.

* Electronic address: denis.grebenkov@polytechnique.edu

[1] S. Rice, *Diffusion-Limited Reactions* (Elsevier, Amsterdam, 1985).

[2] D. A. Lauffenburger and J. Linderman, *Receptors: Models for Binding, Trafficking, and Signaling* (Oxford University Press, 1993).

[3] A. V. Barzykin, K. Seki, and M. Tachiya, "Kinetics of diffusion-assisted reactions in microheterogeneous systems", Adv. Coll. Int. Sci. **89-90**, 47-140 (2001).

[4] R. Metzler, G. Oshanin, S. Redner (Eds.) *First-Passage Phenomena and Their Applications* (World Scientific Press, 2014).

[5] K. Lindenberg, R. Metzler, and G. Oshanin (Eds.) *Chemical Kinetics: Beyond the Textbook*, (World Scientific, 2019).

[6] D. J. Jeffrey, "Conduction through a random suspension of spheres", Proc. R. Soc. Lond. A **335**, 355-367 (1973).

[7] R. F. Kayser and J. B. Hubbard, "Diffusion in a Medium with a Random Distribution of Static Traps", Phys. Rev. Lett. **51**, 79 (1983).

[8] R. F. Kayser and J. B. Hubbard, "Reaction diffusion in a medium containing a random distribution of nonoverlapping traps", J. Chem. Phys. **80**, 1127 (1984).

[9] B. U. Felderhof, "Wigner solids and diffusion controlled reactions in a regular array of spheres," Physica A **130**, 34-56 (1985).

[10] K. Mattern and B. U. Felderhof, "Rate of diffusion-controlled reactions in a random array of spherical sinks," Physica A **143**, 1-20 (1987).

[11] S. Torquato, "Concentration dependence of diffusion-controlled reactions among static reactive sinks", J. Chem. Phys. **85**, 7178 (1986).

[12] P. M. Richards and S. Torquato, "Upper and lower bounds for the rate of diffusion-controlled reactions", J. Chem. Phys. **87**, 4612 (1987).

[13] J. Rubinstein and S. Torquato, "Diffusion-controlled reactions: Mathematical formulation, variational principles, and rigorous bounds", J. Chem. Phys. **88**, 6372 (1988).

[14] S. Torquato, "Diffusion and reaction among traps: some theoretical and simulation results", J. Stat. Phys. **65**, 1173 (1991).

[15] S. Torquato and C. L. Y. Yeong, "Universal scaling for diffusion-controlled reactions among traps", J. Chem. Phys. **106**, 8814 (1997).

[16] A. R. Kansal and S. Torquato, "Prediction of trapping rates in mixtures of partially absorbing spheres", J. Chem. Phys. **116**, 10589 (2002).

[17] A. M. Berezhkovskii and Yu. A. Makhnovskii, "Mutual influence of traps on the death of a Brownian particle," Chem. Phys. Lett. **175**, 499 (1990).

[18] A. M. Berezhkovskii, Yu. A. Makhnovskii, R. A. Suris, L. V. Bogachev, and S. A. Molchanov, "Diffusion-limited reactions with correlated traps", Chem. Phys. Lett. **193**, 211 (1992).

[19] A. M. Berezhkovskii, Yu. A. Makhnovskii, R. A. Suris, L. V. Bogachev, and S. A. Molchanov, "Trap correlation influence on diffusion-limited process rate", Phys. Rev. A **45**, 6119 (1992).

[20] Yu. A. Makhnovskii, A. M. Berezhkovskii, L. V. Bogachev, and S. A. Molchanov, "Brownian-particle trapping by clusters of traps", Phys. Rev. E **47**, 4564 (1993).

[21] G. Oshanin and A. Blumen, "Kinetic description of diffusion-limited reactions in random catalytic media", J. Chem. Phys. **108**, 1140 (1998).

[22] Yu. A. Makhnovskii, A. M. Berezhkovskii, S.-Y. Sheu, D.-Y. Yang, and S. H. Lin, "Role of trap clustering in the trapping kinetics", J. Chem. Phys. **111**, 711 (1999).

[23] Yu. A. Makhnovskii, S.-Y. Sheu, D.-Y. Yang, and S. H. Lin, "Effect of polydispersity on Brownian-particle trapping by clusters of traps", J. Chem. Pyhs. **117**, 897 (2002).

[24] S. D. Traytak, "Competition effects in steady-state diffusion-limited reactions: Renormalization group approach", J. Chem. Phys. **105**, 10860 (1996).

[25] S. D. Traytak, "Convergence of a reflection method for diffusion-controlled reactions on static sinks", Physica A **362**, 240-248 (2006).

[26] M. O. Lavrentovich, J. H. Koschwanez, and D. R. Nelson, "Nutrient Shielding in Clusters of Cells", Phys. Rev. E **87**, 062703 (2013).

[27] S. D. Traytak, "Ligand binding in a spherical region randomly crowded by receptors", Phys. Biol. **10**, 045009 (2013).

[28] F. Piazza and S. D. Traytak, "Diffusion-influenced reactions in a hollow nano-reactor with a circular hole", Phys. Chem. Chem. Phys. **17**, 10417 (2015).

[29] M. Galanti, D. Fanelli, S. D. Traytak, and F. Piazza, "Theory of diffusion-influenced reactions in complex geometries", Phys. Chem. Chem. Phys. **18**, 15950-15954 (2016).

[30] M. Galanti, D. Fanelli, S. Angioletti-Uberti, M. Ballauff, J. Dzubiella, and F. Piazza, "Reaction rate of a composite core-shell nanoreactor with multiple nanocatalysts", Phys. Chem. Chem. Phys. **18**, 20758-20767 (2016).

[31] D. S. Grebenkov and S. Traytak, "Semi-analytical computation of Laplacian Green functions in three-dimensional domains with disconnected spherical boundaries", J. Comput. Phys. **379**, 91-117 (2019).

[32] S. B. Lee, I. C. Kim, C. A. Miller, and S. Torquato, "Random-walk simulation of diffusion-controlled processes among static traps", Phys. Rev. B **39**, 11833 (1989).

[33] H.-K. Tsao, S.-Y. Lu, and C.-Y. Tseng, "Rate of diffusion-limited reactions in a cluster of spherical sinks", J. Chem. Phys. **115**, 3827 (2001).

[34] C. Eun, P. M. Kekenes-Huskey, and J. A. McCammon, "Influence of neighboring reactive particles on diffusion-limited reactions", J. Chem. Phys. **139**, 044117 (2013).

[35] C. Eun, "Effects of the Size, the Number, and the Spatial Arrangement of Reactive Patches on a Sphere on Diffusion-Limited Reaction Kinetics: A Comprehensive Study", Int. J. Mol. Sci. **21**, 997 (2020).

[36] E. A. Ivanov, *Diffraction of Electromagnetic Waves on Two Bodies* (National Aeronautics and Space Administration, Springfield, WA, 1970).

[37] P. A. Martin, *Multiple Scattering: Interaction of Time-Harmonic Waves with N Obstacles* (Cambridge University Press, 2006).

[38] S. Koc and W. C. Chew, "Calculation of acoustical scattering from a cluster of scatterers", J. Acoust. Soc. Am. **103**, 721-734 (1998).

[39] N. A. Gumerov and R. Duraiswami, "Computation of scattering from N spheres using multipole reexpansion", J. Acoust. Soc. Am. **112**, 2688-2701 (2002).

[40] N. A. Gumerov and R. Duraiswami, "Computation of scattering from clusters of spheres using the fast multipole method", J. Acoust. Soc. Am. **117**, 1744-1761 (2005).

[41] F. C. Goodrich, "On the diffusion field in the neighborhood of two identical spheres," Colloid Polym. Sci. **219**, 156-159 (1967).

[42] S. D. Traytak, "The diffusive interaction in diffusion-limited reactions: the steady-state case", Chem. Phys. Lett. **197**, 247-254 (1992).

[43] H.-K. Tsao, "Competitive diffusion into two reactive spheres of different reactivity and size", Phys. Rev. E **66**, 011108 (2002).

[44] N. McDonald and W. Strieder, "Diffusion and reaction for a spherical source and sink", J. Chem. Phys. **118**, 4598 (2003).

[45] S. D. Traytak and D. S. Grebenkov, "Diffusion-influenced reaction rates for active 'sphere-prolate spheroid' pairs and Janus dimers", J. Chem. Phys. **148**, 024107 (2018).

[46] J. T. Chen, K. H. Chou, and S. K. Kao, "Derivation of Green's function using addition theorem," Mech. Res. Commun. **36**, 351-363 (2009).

[47] S. D. Traytak, "On the time-dependent diffusive interaction between stationary sinks", Chem. Phys. Lett. **453**, 212-216 (2008).

[48] E. Gordeliy, S. L. Crouch, and S. G. Mogilevskaya, "Transient heat conduction in a medium with multiple spherical cavities", Int. J. Numer. Meth. Engng **77**, 751-775 (2009).

[49] E. W. Hobson, *The theory of spherical and ellipsoidal harmonics* (New York, Chelsea Publ. Company, 1965).

[50] M. A. Epton and B. Dembart, "Multipole translation theory for the three-dimensional Laplace and Helmholtz equations," SIAM J. Sci. Comput. **16**, 865-897 (1995).

[51] D. Duffy, *Green's functions with applications* (Chapman & Hall/CRC, Boca Raton, 2001).

[52] J. Keilson, *Green's function methods in probability theory* (Hafner, 1965).

[53] C. W. Gardiner, *Handbook of stochastic methods for physics, chemistry and the natural sciences* (Springer: Berlin, 1985).

[54] D. S. Grebenkov, "Imperfect Diffusion-Controlled Reactions", in *Chemical Kinetics: Beyond the Textbook*, Eds. K. Lindenberg, R. Metzler, and G. Oshanin (World Scientific, 2019).

[55] W. Arendt, A. F. M. ter Elst, J. B. Kennedy, and M. Sauter, "The Dirichlet-to-Neumann operator via hidden compactness", J. Funct. Anal. **266**, 1757-1786 (2014).

[56] D. Daners, "Non-positivity of the semigroup generated by the Dirichlet-to-Neumann operator", Positivity **18**, 235-256 (2014).

[57] W. Arendt and A. F. M. ter Elst, "The Dirichlet-to-Neumann Operator on Exterior Domains", Potential Anal. **43**, 313-340 (2015).

[58] A. Hassell and V. Ivrii, "Spectral asymptotics for the semi-classical Dirichlet to Neumann operator", J. Spectr. Theory **7**, 881-905 (2017).

[59] A. Girouard and I. Polterovich, "Spectral geometry of the Steklov problem", J. Spectr. Theory **7**, 321-359 (2017).

[60] D. S. Grebenkov, "Spectral theory of imperfect diffusion-controlled reactions on heterogeneous catalytic surfaces", J. Chem. Phys. **151**, 104108 (2019).

[61] D. S. Grebenkov, "Probability distribution of the boundary local time of reflected Brownian motion in Euclidean domains," Phys. Rev. E **100**, 062110 (2019).

[62] D. S. Grebenkov, "Scaling Properties of the Spread Harmonic Measures", Fractals **14**, 231-243 (2006).

[63] D. S. Grebenkov, "Analytical representations of the spread harmonic measure", Phys. Rev. E **91**, 052108 (2015).

[64] F. C. Collins and G. E. Kimball, "Diffusion-controlled reaction rates", J. Coll. Sci. **4**, 425 (1949).

[65] M. Smoluchowski, "Versuch einer Mathematischen Theorie der Koagulations Kinetic Kolloider Lösungen", Z. Phys. Chem. **129**, 129-168 (1917).

[66] H. Sano and M. Tachiya, "Partially diffusion-controlled recombination", J. Chem. Phys. **71**, 1276 (1979).

[67] C. Y. Son, J. Kim, J.-H. Kim, J. S. Kim, and S. Lee, "An accurate expression for the rates of diffusion-influenced bimolecular reactions with long-range reactivity"m J. Chem. Phys. **138**, 164123 (2013).

[68] K. Lee, J. Sung, C. H. Choi, and S. Lee, "Green's function of the Smoluchowski equation with reaction sink: Application to geminate and bulk recombination reactions", J. Chem. Phys. **152**, 134102 (2020).

[69] M. Lange, M. Kochugaeva, and A. B. Kolomeisky, "Dynamics of the Protein Search for Targets on DNA in the Presence of Traps", J. Phys. Chem. B **119**, 12410-12416 (2015).

[70] D. S. Grebenkov and J.-F. Rupprecht, "The escape problem for mortal walkers", J. Chem. Phys. **146**, 084106 (2017).

[71] D. S. Grebenkov, "NMR Survey of Reflected Brownian Motion", Rev. Mod. Phys. **79**, 1077-1137 (2007).

[72] S. B. Yuste, E. Abad, and K. Lindenberg, "Exploration and trapping of mortal random walkers", Phys. Rev. Lett. **110**, 220603 (2013).

[73] B. Meerson and S. Redner, "Mortality, redundancy, and diversity in stochastic search", Phys. Rev. Lett. **114**, 198101 (2015).

[74] Z. Schuss, K. Basnayake, and D. Holcman, "Redundancy principle and the role of extreme statistics in molecular and cellular biology", Phys. Life Rev. **28**, 52-79 (2019).

[75] J. Lin, C. S. Chen, and C.-S. Liu, "Fast Solution of Three-Dimensional Modified Helmholtz Equations by the Method of Fundamental Solutions", Commun. Comput. Phys. **20**, 512-533 (2016).

[76] W. C. Chew, "Recurrence relations for three-dimensional scalar addition theorem," J. Electromagn. Waves Appl. **6**, 133-142 (1992).

[77] R. Coifman, V. Rokhlin, and S. Wandzura, "The fast multipole method for the wave equation: a pedestrian prescription," IEEE Trans. Antennas Propag. **35**, 7-12 (1993).

[78] E. Darve, "The fast multipole method: a numerical implementation," J. Comput. Phys. **160**, 195-240 (1990).

[79] L. Greengard, V. Rokhlin, "A new version of the fast multipole method for the Laplace equation in three dimensions," Acta Numer. **6**, 229-269 (1997).

[80] H. W. Cheng, W. Y. Crutchfield, Z. Gimbutas, L. F. Greengard, J. F. Ethridge, J. Huang, V. Rokhlin, N. Yarvin, and J. Zhao, "A wideband fast multipole method for the Helmholtz equation in three dimensions," J. Comput. Phys. **216**, 300-325 (2006).

[81] A. Hesford, J. P. Astheimer, L. Greengard, and R. Wang, "A mesh-free approach to acoustic scattering from multiple spheres nested inside a large sphere using diagonal translation operators," J. Acoust. Soc. Am. **127**, 850-861 (2010).

[82] V. T. Erofeenko, *Addition theorems* (Minsk, Nauka i Texnika, 1989) [in Russian].

[83] N. Agmon and A. Szabo, "Theory of reversible diffusion-influenced reactions", J. Chem. Phys. **92**, 5270 (1990).

[84] M. Tachiya, "Theory of diffusion-controlled dissociation and its applications to charge separation," in Extended Abstract of Annual Meeting on Photochemistry, Tsu, Japan, 1980 (Japan. Photochem. Assoc., 1980), pp. 256-257.

[85] N. Agmon, "Diffusion with back reaction", J. Chem. Phys. **81**, 2811 (1984).

[86] H. Kim and K. J. Shin, "Exact Solution of the Reversible Diffusion-Influenced Reaction for an Isolated Pair in Three Dimensions", Phys. Rev. Lett. **82**, 1578 (1999).

[87] T. Prüstel and M. Tachiya, "Reversible diffusion-influenced reactions of an isolated pair on some two dimensional surfaces", J. Chem. Phys. **139**, 194103 (2013).

[88] D. S. Grebenkov, "Reversible reactions controlled by surface diffusion on a sphere", J. Chem. Phys. **151**, 154103 (2019).

[89] G.-W. Li, O. G. Berg, and J. Elf, "Effects of macromolecular crowding and DNA looping on gene regulation kinetics", Nature Phys. **5**, 294 (2009).

[90] O. Bénichou, Y. Kafri, M. Sheinman, and R. Voituriez, "Searching Fast for a Target on DNA without Falling to Traps", Phys. Rev. Lett. **103**, 138102 (2009).

[91] P. C. Bressloff and J. M. Newby, "Stochastic models of intracellular transport", Rev. Mod. Phys. **85**, 135-196 (2013).

[92] B. Friedman and J. Russek, "Addition theorems for spherical waves", Quart. Appl. Math. **12**, 13-23 (1954).

[93] M. Abramowitz and I. A. Stegun, *Handbook of Mathematical Functions* (Dover Publisher, New York, 1965).

[94] N. A. Gumerov and R. Duraiswami, "Fast, Exact, and Stable Computation of Multipole Translation and Rotation Coefficients for the 3-D Helmholtz Equation," University of Maryland Institute for Advanced Computer Studies Technical Report UMIACS-TR-#2001-44 (2001) [Available at http://users.umiacs.umd.edu/~ramani/pubs/multipole.pdf]

[95] D. S. Grebenkov, R. Metzler, and G. Oshanin, "Strong defocusing of molecular reaction times results from an interplay of geometry and reaction control", Commun. Chem. **1**, 96 (2018).